NASA CONTRACTOR REPORT

NASA CR-9

NASA CR-905

TRANSIENT RADIATION AND CONDUCTION IN A SLOTTED SLAB AND A HOLLOW CYLINDER

by P. D. Richardson and Y.-M. Shum

Prepared by
BROWN UNIVERSITY
Providence, R. I.
for

NATIONAL AERONAUTICS AND SPACE ADMINISTRATION • WASHINGTON, D. C. • OCTOBER 1967

NASA CR-905

TRANSIENT RADIATION AND CONDUCTION IN A SLOTTED SLAB AND A HOLLOW CYLINDER

By P. D. Richardson and Y.-M. Shum

Prepared under Grant No. NGR-40-002-012 by
BROWN UNIVERSITY
Providence, R.I.

for

NATIONAL AERONAUTICS AND SPACE ADMINISTRATION

For sale by the Clearinghouse for Federal Scientific and Technical Information
Springfield, Virginia 22151 – CFSTI price $3.00

TRANSIENT RADIATION AND CONDUCTION IN A SLOTTED SLAB AND A HOLLOW CYLINDER

P. D. RICHARDSON[1] and Y.-M. SHUM[2]

DIVISION OF ENGINEERING, BROWN UNIVERSITY

PROVIDENCE, RHODE ISLAND

Temperature distributions in a parallel-walled channel (a typical slot in a slotted slab) and in a hollow cylinder are considered. Each end of the channel or cylinder faces an environment of uniform but alterable temperature. Black wall surfaces are assumed, and for most solutions presented the radiant heat flux is linearized with respect to temperature. Transient solutions are obtained for cases where the walls are thin, and where they are (thermally) thick; in the latter case, transient conduction normal to the wall surfaces is coupled into the problem. Examples of superposition are given. For the hollow cylinder, prescribed heat generation along the wall is also treated. The concept of the radiation mean free effective path is found to be useful. Generalization to non-black surfaces is discussed.

---

[1]Associate Professor

[2]Research Assistant

CONTENTS

1. INTRODUCTION

Thermal radiation in cavities and enclosures has been a problem of practical importance for many years, the principal interest being furnace design and operation. More recently, many new practical examples of radiation in cavities and enclosures have arisen; aerospace vehicle structures, the surface structure of the moon and other bodies in the solar system, and the solid core of a gaseous-fuelled nuclear propulsion reactor are typical. Radiation heat exchangers are important for heat rejection from power-generating space vehicles, and it is plausible that some use may be found for radiation regenerators.

In general, the formulation of a radiant interchange problem requires the use of an energy balance at points within a region of an absorbing and emitting continuum or at points on opaque surfaces, and this energy balance leads to an integro-differential equation for the local temperature or heat flux, whichever is unknown. Because of the complexity of the governing equations, a closed-form analytical solution can only rarely be obtained. Consequently, it is common to employ numerical techniques or various approximate analytical approaches. For example, for problems which involve radiant interchange between surfaces of steady but non-uniform temperature distribution, Sparrow and Haji-Sheikh [1] applied a variational method, while Keshock and Siegel [2] used an iteration technique, and Viskanta [3] has suggested the method of successive substitutions to obtain solutions for the same problem. Usiskin and Siegel [4] also obtained approximate solutions for steady-state-radiation in a finite tube by three different methods: use of an approximate separable kernel, numerical integration and a variational method.

The more general problem where the temperature of bodies involved in radiant interchange is considered to vary not only with position but also with time has received very little attention. Winter [5] recently has presented results from a computed solution based on a finite-difference method for a restricted class of problems involving a semi-infinite slotted slab.

The principal objective of the present investigation is to look more generally at problems involving transient combined radiative interchange and conduction. Considerations have been restricted to simple geometries--slotted slabs and hollow cylinders (or holes in slabs), but for slabs of finite thickness as well as the semi-infinite configuration. Attention is concentrated here on the cases which permit use of approximate analytical methods. It is to be expected that treatment of cases for the full range of the parameters (which arise naturally for the geometries considered) will involve a combination of numerical and analytical techniques, and indeed the authors have found that a readily usable numerical scheme can be devised. However, the analytical methods used here are important in solution of the general problem because they rapidly provide significant details of the structure of the solutions, and can also be used as (asymptotic) checks on numerical solutions.

The distinguishing characteristic of some particular cases for which approximate analytical techniques can readily be devised is that conduction in the direction normal to the slot side walls (or to the cylinder wall) does not give significant temperature variations. This implies that the walls are thermally thin, i.e. the time for the transient penetration depth to traverse the wall thickness is small

compared with the time-scale of the radiation transient. For the slab, this usually requires that the slot width is much greater than the wall thickness (as in a set of fins). The results can also be applied to thick-walled situations. For thin-wall circumstances, radiation is the dominant mode of energy transfer. At short times after the initiation of a transient, the change in wall temperature is governed by radiative transfer and is linearly proportional to time. With thermally thick walls, the local temperature change is initially proportional to the square-root of time. At longer times, and in the steady-state, longitudinal conduction can become more significant; its effect is to reduce temperature gradients. In the course of the analysis it is found possible to evoke the concepts of photon mean free effective path, radiation conductivity and diffusivity and to use these in defining dimensionless variables in terms of which the pertinence of the solutions to particular physical problems can be assessed.

2. STATEMENT OF THE PROBLEM

The geometrical systems considered are shown in Fig. 1(a) for a symmetrical component of the slotted slab and in Fig. 1(b) for the hollow cylinder. Throughout this section, the designations (a) and (b) given to equations are appropriate to the respective geometries. The two parallel plates which constitute the typical component of the slotted slab are infinitely wide, and have a separation a and a length L in the x-direction. By symmetry, it is assumed that the outer surfaces of the plates, away from the slot, are adiabatic (these surfaces represent the mid-planes of the plates in a repeatedly slotted slab). For the cylindrical case the outer surface is also considered adiabatic. For both geometries, the inner surfaces are assumed black. It is also assumed that each end of the slot or cylinder sees a uniform external environment, such that the radiation properties can be represented by a black isothermal plane covering each end.

Transient solutions can be obtained for a large set of initial and boundary conditions. With radiation in the problem, the governing equation is not linear in temperature and superposition is not formally justified as a means for constructing solutions for complex initial and boundary conditions. (Nevertheless, superposition can often give a good approximation.) The conditions chosen here are that the system is initially at a uniform temperature T_i ; then, at time $t = 0$, there is a step change of environment temperature from T_i to T_o at one end of the slot (or tube), with $T_o < T_i$.

The energy balance equation is formed for unit length of a typical elemental strip on the plates (or for an elemental ring in the

cylinder). By consideration of the radiation from the element, its change in internal energy, conduction along the wall, and the radiant transfer from the end planes and from other elementary surfaces of the wall surface, the following nonlinear integro-differential equations are obtained:

$$\sigma T_1^4(x_1,t) + \delta\rho c \frac{\partial T_1(x_1,t)}{\partial t} - \delta k \frac{\partial^2 T_1(x_1,t)}{\partial x_1^2} = \tag{1a}$$

$$= \sigma T_i^4(F(x_1) + \sigma T_o^4 F(L - x_1) + \int_0^L \sigma T_2^4(x_2,t)\, E\,(|x_1 - x_2|)\, dx_2$$

$$\sigma T_1^4(x_1,t) + \delta\rho c \frac{\partial T_1(x_1,t)}{\partial t} + \delta k \frac{\partial^2 T_1(x_1,t)}{\partial x_1^2} = \tag{1b}$$

$$= \sigma T_i^4 F\left(\frac{x_1}{D}\right) + \sigma T_o^4 F\left(\frac{L - x_1}{D}\right) + \int_0^L T_2^4(x_2,t)\, K\left(\frac{|x_1 - x_2|}{D}\right) d\left(\frac{x_2}{D}\right)$$

Since the walls have been assumed thin, as explained earlier, radiant interchange between the end surfaces of the plates (or tube), at $x = 0$ and $x = L$, and the environments is neglected here. The initial and boundary conditions are that

$$\begin{aligned} T(x_1,0) &= T_i \\ T = T_i \quad &\text{for} \quad t > 0 \quad \text{and} \quad x_1 = 0^- \\ T = T_o \quad &\text{for} \quad t > 0 \quad \text{and} \quad x_1 = L^+ \end{aligned} \tag{2}$$

It must be realized that $T(0,t)$ and $T(L,t)$ are not equal to T_i and T_o respectively, but are determined as part of the solution of eqn. (1).

The angle factor $F(x_j)$ for the planes is given by Hottel and Keller [6] as

$$F(x_j) = \frac{1}{2}\{1 - x_j/(x_j^2 + a^2)^{1/2}\} \tag{3a}$$

and $E(|x_1 - x_2|)$ is

$$E(x_j) = \frac{1}{2} a^2/(x_j^2 + a^2)^{3/2} \ . \tag{4a}$$

The corresponding factors for the cylinder are given by Buckley [7] as

$$F(x_j) = \frac{x_j^2 + 1/2}{(x_j^2 + 1)^{1/2}} - x_j \ , \quad x_j \geq 0 \tag{3b}$$

and

$$K(x_j) = 1 - \frac{x_j^3 + 3x_j/2}{(x_j^2 + 1)^{3/2}} \ , \quad x_j \geq 0 \tag{4b}$$

The equations can be expressed in terms of dimensionless variables

$$\begin{aligned} T^* &= T/T_i \\ \tau &= t/(\delta\rho c/\sigma T_i^3) \\ \nu &= a/L \end{aligned} \tag{5}$$

$$\begin{aligned} z &= x_1/L \\ \xi &= x_2/L \end{aligned} \tag{5a}$$

$$\begin{aligned} \ell &= L/D \\ z &= x_1/D \\ \xi &= x_2/D \end{aligned} \tag{5b}$$

such that eqn. (1) becomes

$$T^{*4}(z,\tau) = \frac{1}{2}\left[1 - \frac{z}{(\nu^2 + z^2)^{1/2}}\right] + \frac{T_o^{*4}}{2}\left[1 - \frac{1 - z}{\{\nu^2 + (1 - z)^2\}^{1/2}}\right] +$$

$$+ \int_0^1 T^{*4}(\xi,\tau) \frac{\nu^2 d\xi}{2[(z - \xi)^2 + \nu^2]^{3/2}} - \frac{\partial T^*(z,\tau)}{\partial \tau} + \tag{6a}$$

$$+ \frac{k\delta}{\sigma T_i^3 L^2} \frac{\partial^2 T^*(z,\tau)}{\partial z^2}$$

and, correspondingly,

$$T^{*4}(z,\tau) = F(z) + T_o^{*4}F(\ell - z) + \int_0^{\ell} T^{*4}(\xi,\tau)\, K(|z - \xi|)\, d\xi - \frac{\partial T^*(z,\tau)}{\partial \tau} + \frac{k\delta}{\sigma T_i^3 L^2} \cdot \frac{\partial^2 T^*(z,\tau)}{\partial z^2} \quad . \tag{6b}$$

The initial and boundary conditions transform to

$$\tau = 0, \quad T^* = 1;$$

$$z = 0^-, \quad T^* = 1, \quad \text{for } \tau > 0,$$

$$z = 1^+ \quad \text{(plates)}$$

$$z = \ell^+ \quad \text{(cylinder)} \qquad T^* = T_o^* \quad \text{for } \tau > 0 .$$

From this point it is most convenient to separate the discussion of the two geometries. However, the treatments given here are interleaved because features found in solutions for one geometry are broadly applicable to the other geometry, and undue repetition of physical interpretations and of examples can be avoided.

2.1 The photon mean free effective path

A concept which can be used in both the cylindrical and plate geometries is the mean free effective apth. To define this, it is desirable to consider that $L \to \infty$ and to center attention on an emitting elementary surface on the wall. Photons emitted from this elementary surface strike other parts of the walls and are absorbed. For the parallel plates this absorption occurs on the opposite plate; in the cylinder it can occur anywhere except on the same generator as the emitting element. For the problems considered here, radiant transfer

in the x-direction is significant; symmetry of initial and boundary conditions in the directions orthogonal to x has assured that transverse variations are absent. Since x is the direction significant for net radiation flux, the component of a photon path in the x-direction can be considered the effective path. Further, since the problem is concerned with net radiation flux in the x-direction, it is pertinent to consider photons emitted from the element in the positive direction, say, and to ignore those emitted in the opposite direction. The photon effective path then varies from zero to infinity. However, a mean free effective path can be defined by weighting each effective path by the proportion of the total photons emitted which take that path. Thus for long plates the mean free effective path is a, and for long cylinders it is $D/2$.

Generalization of this concept to other geometrical configurations and to non-black surfaces is discussed in Section 6.

3. STEADY STATE SOLUTIONS

When time t becomes very large, the temperature distributions can be expected to settle to values essentially independent of t. In this section the solutions of eqns. (6a) and (6b), reduced by removal of the transient term, are discussed.

3.1 The cylindrical geometry

The steady-state solution for this case can be investigated very readily if the axial conduction term is dropped from the equation. When this is done, the local energy balance equation (6b) becomes

$$T^{*4}(z) = F(z) + T_o^{*4} F(\ell - z) + \int_0^{\ell} T^{*4}(\xi) K(|z - \xi|) \, d\xi \qquad (7)$$

with boundary conditions

$$\begin{aligned} &x = 0^-, \quad T^* = 1 \\ \text{and} \quad &x = \ell^+, \quad T^* = T_o^* . \end{aligned} \qquad (8)$$

Usiskin and Siegel [4] have shown that the angle factor $F(z)$ can be approximated by $(1/2)\exp(-2z)$, and Buckley [7] demonstrated that the kernel K can be approximated by $\exp(-2z)$. Usiskin and Siegel used these approximations to obtain an analytic solution:

$$T^{*4} = T_o^{*4} + (1 - T_o^{*4})(c_1 - c_2 z) \qquad (9)$$

where $$c_1 = \frac{1/2 + \ell}{1 + \ell} = 1 - 1/2(1 + \ell)$$

and $$c_2 = 1/(1 + \ell) . \qquad (10)$$

This solution serves to illustrate typical steady state results. The temperature distribution along the tube is approximately linear in T^4;

there are temperature defferences between the ends and the reservoirs at T_i and T_o. Figure 2 illustrates T/T_i vs. x/L for $\ell = 1, 2, 5$ and 10, for the extreme case $T_o = 0$. The axial temperature distribution is close to linear except when ℓ becomes large. Figure 3 shows how the total heat flux through the tube is affected by ℓ ; the part of the flux which goes straight through is shown as a dashed line. The heat flux which goes straight through decreases very rapidly with increase in ℓ because the cylinder walls intercept a large solid angle of the total, hemispherical radiation from points on the end plane. For small ℓ , much of the once-absorbed radiation is re-emitted without repeated capture on the cylinder walls, but by $\ell = 2$ the majority of the heat flux is transmitted by multiple absorption and re-emission. If an analogy is made with radiation in gases, $\ell > 2$ corresponds to an optically thick gas layer. When $\ell \to \infty$, $c_1 \to 1$ and $c_2 \to 1/\ell$, which gives the same temperature distribution as would be found in the Rosseland limit for a grey gas. When ℓ is large but finite, the solution is similar to that in a gas with radiation "slip" [8] at $z = 0$, $z = \ell^+$.

The overall net heat flux can be expressed as

$$\frac{\dot{Q}_{i \to 0}}{\pi R^2 \sigma (T_i^4 - T_o^4)} = 2\left[\ell^2 + (1/2) - \left((\ell^2 + 1/2)^2 - 1/4\right)^{1/2}\right] +$$

$$+ 4\left\{c_1\left[(\ell/2)(\ell^2 + 1)^{1/2} - \ell^2/2\right] +\right.$$

$$\left. + (c_2/6)\left[(\ell^2 + 1)^{3/2} - 1 - \ell^3\right]\right\} . \qquad (11)$$

3.2 The hollow cylinder with distributed heat sources

It is possible to extend the solution given in Section 3.1 to include the effects of a specified heat source distribution along the wall. If this heat source is azimuthally uniform, it can be represented by a term $q(x)/\sigma T_i^4$, giving the heat flux density at x, added to the right-hand side of eqn. (7). This form of the energy equation is still linear in T^{*4}, and a solution to the equation with distributed heat sources can be obtained by superposition, i.e.

$$T^{*4}(z) = T_o^{*4} + (1 - T_o^{*4})(c_1 - c_2 z) + T_q^{*4}(z) \qquad (12)$$

where $T_q^*(z)$ is the solution of the amended eqn. (7) with boundary conditions that the reservoir temperatures at both ends of the cylinder are zero. A variational method can be introduced to obtain the solution for $T_q^*(z)$.

Let $B(z) = T_q^4(z)$, and $\phi(z) = q(z)/\sigma$. A variational expression for $B(z)$ can be found as

$$I_q = \int_0^\ell \int_0^\ell K(|z - \xi|)\, B(z)\, B(\xi)\, dz d\xi - \int_0^\ell B^2(z)\, dz + 2 \int_0^\ell B(z)\, \phi(z)\, dz , \qquad (13)$$

and a solution obtained using the rational expression for K, eqn. (4b). A solution for this problem can be obtained more expeditiously by further use of the approximation $K(x_j) = \exp(-2x_j)$, i.e.

$$B(z) = \int_0^z B(\xi) \exp(-2(z - \xi))\, d\xi + \int_z^\ell B(\xi) \exp(-2(\xi - z)) d\xi + \phi(z)$$

$$= e^{-2z} \int_0^z B(\xi) e^{2\xi}\, d\xi + e^{2z} \int_z^\ell B(\xi) e^{-2\xi}\, d\xi + \phi(z) .$$

The integrals can be removed by double differentiation, after which a

simple differential equation is obtained

$$\frac{d^2B}{dz^2} = \frac{d^2\phi}{dx^2} - 4\phi$$

so that

$$B(z) = az + b + \phi(z)$$

where

$$\phi(z) = \int_z \int_\xi \left(\frac{d^2\phi}{dz^2} - 4\phi\right) dz\, d\xi \qquad (14)$$

and a and b are constants of integration determined from the boundary conditions:

$$\text{at} \quad x = 0, \quad B(0) = b + \phi(0);$$

$$\text{also,} \quad B(0) = \int_0^\ell B(\xi)\, e^{-2\xi} d\xi + \phi(0)$$

$$\text{so that} \quad b + \phi(0) = \int_0^\ell [a\xi + b + \phi(\xi)]\, e^{-2\xi} d\xi + \phi(0).$$

Similarly, for $x = \ell$,

$$a\ell + b + \phi(\ell) = e^{-2\ell} \int_0^\ell [a\xi + b + \phi(\xi)]\, e^{-2\xi}\, d\xi + \phi(\ell).$$

From these relations, a and b can be determined once $\phi(z)$ is specified. This can be illustrated by two examples:

(i) $q(z) = \text{constant} = Q,$

so that $\phi = Q/\sigma$

$\phi(z) = -(2Q/\sigma)z^2$

and $a = (2Q/\sigma)\ell, \quad b = (1 + \ell)(Q/\sigma),$

whence

$$B(z) = T^4(z) = (Q/\sigma)\,[1 + \ell + 2x(\ell - x)]. \qquad (15)$$

(ii) $q(z) = Qz$

so that $\phi(z) = Qz/\sigma$,

$\Phi(z) = -(2Q/3\sigma)z^3$,

$a = (Q/3\sigma)(2\ell^3 + 3\ell^2 + 3\ell + 3)/(\ell + 1)$

and $b = (Q/6\sigma)\ell^2(2\ell + 3)/(\ell + 1)$,

whence

$$T^4(z) = \left(\frac{Q}{3\sigma}\right)\left\{\frac{(2\ell^3 + 3\ell^2 + 3\ell + 3)z}{\ell + 1} + \frac{1}{2}\frac{\ell^2(2\ell + 3)}{\ell + 1} - 2z^3\right\} \quad (16)$$

The consequent temperature distributions for examples (i) are illustrated in Figure 4, for various ℓ, for the case $Q/\sigma = T_i^4$.

3.3 The plate geometry

The steady-state solution for this case is considered here with inclusion of the heat conduction term. Obviously, this will render the energy balance equation no longer linear in T^4, but it is convenient to work with linear equations. This is still a reasonable possibility if $[1 - T^{*4}(z)] << 1$. The departure from effective linearityof this sort in the previous solution (Section 3.1) was slight, except at the cold end for large ℓ, so linearization may be introduced: let

$$T^* = 1 - T^+ \quad (17)$$

and let it be assumed that T^+ is a small perturbation, so that

$$T^{*4} \approx 1 - 4T^+$$

By substituting eqn. (17) into eqn. (6a) and omitting the time-dependent term, it is found that

$$T^+(z) = (1/8)(1 - T_o^{*4}) \left\{ 1 - \frac{1 - z}{[\nu^2 + (1 - z)^2]^{1/2}} \right\} +$$

$$+ \int_0^1 \frac{T^+(\xi)}{2} \frac{\nu^2 d\xi}{[(z - \xi)^2 + \nu^2]^{3/2}} + \lambda_k \frac{\partial^2 T^+(z)}{\partial z^2} \qquad (18)$$

where

$$\lambda_k = k\delta/(4\sigma T_i^3 L^2) \ . \qquad (19)$$

The boundary conditions are

$$z = 0^-, \ T^+ = 0$$
$$z = 1^+, \ T^+ = 1 - T_0^* \qquad (20)$$

Equation (18) is of the form

$$\phi_1(z) = \psi_1(z) + \int_0^1 \phi_2(\xi) K_{1,2} \, d\xi + \lambda \frac{d^2\phi_1}{dz^2} \qquad (21a)$$

or

$$\phi_2(\xi) = \psi_2(\xi) + \int_0^1 \phi_1(z) K_{2,1} \, dz + \lambda \frac{d^2\phi_2}{d\xi^2} \ . \qquad (21b)$$

It can be shown that the integro-differential equations (21a) and (21b) can be solved by obtaining the extremum of the associated variational principle

$$I = 2 \int_0^1 \int_0^1 \phi_1(z) \, \phi_2(\xi) K_{1,2}(z,\xi) \, dz \, d\xi -$$

$$- \int_0^1 \phi_1^2(z) dz - \int_0^1 \phi_2^2(\xi) \, d\xi +$$

$$+ 2 \int_0^1 \psi_1(z) \, \phi_1(z) dz + 2 \int_0^1 \psi_2(\xi) \, \phi_2(\xi) d\xi -$$

$$- \lambda \int_0^1 \left(\frac{d\phi_1}{dz} \right)^2 dz - \lambda \int_0^1 \left(\frac{d\phi_2}{d\xi} \right)^2 d\xi \ . \qquad (22)$$

It is clear that the functions in (22) can be identified as:

$$\phi_1(z) = T^+(z), \quad \phi_2(\xi) = T^+(\xi),$$

$$\psi(z) = (1/8)(1 - T_o^{*4})\left\{1 - \frac{1 - z}{[\nu^2 + (1 - z)^2]^{1/2}}\right\},$$

$$K_{1,2}(z,\xi) = \nu^2/2[(z - \xi)^2 + \nu^2]^{3/2}$$

and

$$\lambda = \lambda_k \ .$$

Solutions can be obtained with the aid of the variational principle once the class of admitted functions for ϕ_1 and ϕ_2 is selected. Here, it is convenient to consider the most simple form,

$$T^+(z) = c_1 + c_2 z \tag{23}$$

$$T^+(\xi) = c_1 + c_2 \xi \ . \tag{24}$$

Upon substitution of these equations into equation (22), a simple algebraic expression for I is obtained, and equating the differentials of I with respect to c_1 and c_2 to zero gives

$$c_1 = \begin{vmatrix} D_1 & B_1 \\ D_2 & B_2 \end{vmatrix} \Big/ \begin{vmatrix} A_1 & B_1 \\ A_2 & B_2 \end{vmatrix} \tag{25a}$$

$$c_2 = \begin{vmatrix} A_1 & D_1 \\ A_2 & D_2 \end{vmatrix} \Big/ \begin{vmatrix} A_1 & B_1 \\ A_2 & B_2 \end{vmatrix} \tag{25b}$$

where

$$A_1 = 2\alpha_1 - 4, \quad A_2 = A_1/2$$

$$B_1 = A_1/2, \quad B_2 = 2\alpha_2 - 4/3 - 4\lambda_k$$

$$D_1 = (1/2)(1 - T_o^{*4})(\beta_1 - 1)$$

$$D_2 = (1/2)(1 - T_o^{*4})(\beta_2 - \beta_3 - 1/2)$$

and

$$\alpha_1 = 2((\nu^2 + 1)^{1/2} - \nu)$$

$$\alpha_2 = -5\nu/3 + (\nu^2 + 1)^{1/2} + (2\nu/3)(\nu^2 + 1) - \\ -(\nu^2 + 1)^{3/2}/3 - 4\nu^3/3 + \nu^2(\nu^2 + 1)^{1/2}$$

$$\beta_1 = \alpha_1/2, \quad \beta_2 = \sinh^{-1}(1/\nu) - \beta_1$$

and

$$\beta_3 = 2\nu - 3(\nu^2 + 1)^{1/2}/2 + (1/2)(2 - \nu^2)\sinh^{-1}(1/\nu)$$

The accuracy of solutions obtained by a variational method can be improved by assuming T^+ to be a more complicated function of the space coordinate. However, the algebra is already somewhat complicated for the simplest form of T^+; and the solution which has been obtained is not exactly linear in z when transformed back into physical coordinates, since

$$T(z) = T_i[1 - 4T^+(z)]^{1/4} \\ = T_i[1 - 4(c_1 + c_2 z)]^{1/4} \qquad (26)$$

This is illustrated below for a specific example.

The net rate of heat transfer through unit width of channel, corresponding to this temperature distribution, is

$$\frac{\dot{Q}_{i \to o}}{a\sigma T_i^4} = (1 - T_o^{*4})[(\nu^2 + 1)^{1/2} - 1]/\nu + \\ + (1/\nu)\{(1 - 4c_1)(1 + \nu - (\nu^2 + 1)^{1/2}) - \\ - 4c_2[1/2 + \nu - (\nu^2 + 1)^{1/2}/2 - (\nu^2/2)\sinh^{-1}(1/\nu)]\} - \\ - (T_o^{*4}/\nu)(1 + \nu - (\nu^2 + 1)^{1/2}) - 8c_2\lambda_k/\nu \; . \qquad (27)$$

For pure radiation (i.e. no conduction), Sparrow [9] derived the asymptotic

expression for the heat flux through a long channel as

$$\frac{\dot{Q}_{i \to o}}{a\sigma T_i^4} = \nu \ell n(2/\nu) - \nu/2 \ . \qquad (28)$$

Details of the temperature distribution and an indication of the significance of conduction can be obtained once a specific set of physical circumstances is considered. For an illustrative example, the following conditions were used:

δ = 1/8 inch

k = 12 Btu/hr ft °F

ρ = 490 lb/ft^3

c = 0.11 Btu/lb °F

and T_i = 1000 °F = 1460 °R, T_0 = 0 °R

Figure 5 shows $T(z)/T_i$ as a function of z for ν = 0.2 and 1.0. The temperature-levelling effect of the conductivity of the plates is also illustrated. It can be seen that the solution achieves temperature distribution similar in shape to those found for the hollow cylinder without linearization.

4. TRANSIENT SOLUTIONS

For the plates, if

$$\frac{\sigma T_i^3 a^2}{\delta k} >> 1 \tag{29}$$

the steady heat transfer is dominated by the radiation; and if this parameter is significantly smaller than unity, the steady heat transfer is dominated by the longitudinal conduction. It is possible to form a similar expression for the cylinder. The solutions obtained in Section 3 are appropriate for radiation-dominated heat transfer.

It might be thought that the same parameter is appropriate for determining when radiation dominates transient heat transfer as well, because the material in the walls provides the heat capacity on which the diffusivity for both the radiation and the conduction is based. However, if simple lumping of the heat capacity in the walls is to be used in analysis, the pertinent comparison is between the relaxation time for transverse conduction through the wall $(c\rho\delta^2/k)$ and the characteristic penetration time for radiation along the cylinder or channel. For the plates $\tau_{rad} >> \tau_{cond}$ if

$$\frac{\sigma T_i^3 a^2}{\delta k}\left(\frac{\delta^2}{L^2}\right) << 1 . \tag{30}$$

When this is combined with the condition for one-dimensional treatment of the wall in steady conduction, it is clear that $(\delta^2/L^2) <<< 1$ is required. When $\tau_{rad} \simeq \tau_{cond}$, yet (29) is fulfilled, it is to be expected that the initial (short-time) solution for a transient will have to include treatment of the transverse conduction, but that at later times it is acceptable to revert to a one-dimensional treatment. In this section the plane and cylindrical geometries are discussed first under the assumption that both (29) and (30) hold.

4.1 The plate geometry

The equation for local energy balance, subject to the same linearization as in the steady-state problem, is

$$T^+(z,\tau) = (1/8)(1 - T_o^{*4}) \left\{1 - \frac{1 - z}{[\nu^2 + (1 - z)^2]^{1/2}}\right\} +$$

$$+ \int_0^1 T^+(\xi,\tau) \frac{\nu^2 d\xi}{2[(z - \xi)^2 + \nu^2]^{3/2}} +$$

$$+ \lambda_k \frac{\partial^2 T_1^+(z,\tau)}{\partial z^2} - \frac{1}{4} \frac{\partial T^+(z,\tau)}{\partial \tau} \qquad (31)$$

with initial and boundary conditions

$$\begin{aligned} &\tau = 0, \quad T^+ = 0 \\ &z = 0^-, \quad \tau > 0 \quad : \quad T^+ = 0 \\ &z = 1^+, \quad \tau > 0 \quad : \quad T^+ = 1 - T_o^* \end{aligned} \qquad (32)$$

Equation (31) can be put in a more convenient form by multiplying it by $4e^{4\tau}$, and then integrating from 0 to τ, giving

$$T^+(z,\tau) = (1/8)(1 - T_o^{*4}) \left\{1 - \frac{1 - z}{[\nu^2 + (1 - z)^2]^{1/2}}\right\}(1 - e^{-4\tau}) +$$

$$+ \int_0^\tau \int_0^1 4e^{4(s-\tau)} T^+(\xi,\tau) \frac{\nu^2 d\xi}{2[(z - \xi)^2 + \nu^2]^{3/2}} ds +$$

$$+ \lambda_k \int_0^\tau 4e^{4(s-\tau)} \frac{\partial^2 T^+(z,s)}{\partial z^2} ds . \qquad (33)$$

Because of the complexity of this equation, approximate solutions for short and long times only are described here.

4.1.1 Short-time solution

By direct substitution it is possible to obtain an approximate solution valid for short times:

$$T^+(z,\tau) = (1/2)(1 - T_o^{*4})\left\{1 - \frac{1 - z}{[\nu^2 + (1 - z)^2]^{1/2}}\right\}\tau \qquad (34)$$

and

$$T(z,\tau) = T_i[1 - 4T^+(z,\tau)]^{1/4} \qquad (35)$$

Temperature profiles along plates have been plotted on Figure 6 for $\tau = 0.02, 0.05$ and 0.10, for $\nu = 0.2, 0.5$ and 1.0. It can be seen clearly that these profiles are similar to profiles found in other diffusion problems under corresponding boundary conditions. For the case involving the longest plates ($\nu = a/L = 0.2$) the profiles exhibit a penetration depth effect (increasing with time) rather clearly. These profiles also serve to illustrate the utility of obtaining solutions in terms of T^+; because this is the deviation from the initial value, determination of T^+ can give the value of T with considerable precision. Eqn. (34) shows that for $\tau << 1$ the effect of longitudinal conduction is negligible.

4.1.2 Full-range solution

At large values of τ, the solution is affected by the conduction term, just as in steady-state problems. However, the conduction term is dropped here because this considerably facilitates generation of an approximate solution. By the method of successive substitutions it is possible to obtain a solution of eqn. (33), less the conduction term, and valid for the full range of time, as

$$\begin{aligned} T^+(z,\tau) = {} & (1 - e^{-4\tau})(\phi_0(z) + \phi_1(z) + \phi_2(z) + ...) - \\ & - 4\tau e^{-4\tau}(\phi_1(z) + \phi_2(z) + ...) - \\ & - (1/2!)(4\tau)^2 e^{-4\tau}(\phi_2(z) + \phi_3(z) + ...) - \\ & - (1/3!)(4\tau)^3 e^{-4\tau}(\phi_3(z) + ...) - ..... \end{aligned} \qquad (36)$$

where

$$\phi_0(z) = (1/8)(1 - T_o^{*4})\left\{1 - \frac{1 - z}{[\nu^2 + (1 - z)^2]^{1/2}}\right\},$$

$$\phi_n(z) = \frac{1}{2}\int_0^1 \frac{\nu^2 \phi_{n-1}(\xi)d\xi}{[(z - \xi)^2 + \nu^2]^{3/2}}, \quad n > 0 .$$

To evaluate $\phi_n(z)$ numerical methods must be used, except for the case $\nu = \infty$ for which $\phi_o = (1/8)(1 - T_o^{*4})$, $\phi_n = 0$ for $n > 0$.

Figure 7 shows T/T_i at the mid-point along a plate, i.e. at $z = 1/2$ as a function of T_o^* for $\nu = 1$. Figure 8 illustrates the effect of different ν by presenting T/T_i for $\nu = \infty$, 2 and 1 for $T_o = 0$.

4.2 The cylindrical geometry

In the steady-state analysis for heat transfer through a hollow cylinder no linearization was employed. The steady-state and transient analyses for the parallel plates were carried out using linearization, and the results give a posteriori justification to the linearization as a useful approximation. For analysis of a transient in the cylindrical geometry it is useful to employ the same linearization, as this permits demonstration of a Laplace Transform method; because the previous example demonstrated that longitudinal conduction is less important in transient conduction than in steady-state, the conduction term is dropped. The equation for local energy balance becomes

$$T^+(z,\tau) = (1/8)(1 - T_o^{*4})\exp[-2(\ell - z)] + \int_0^{\ell} T(\xi,\tau)\exp[-2|z - \xi|]d\xi - \frac{1}{4}\frac{\partial T(z,\tau)}{\partial \tau} \tag{37}$$

The initial and boundary conditions considered correspond to those used in Section 4.1. If eqn. (37) is differentiated twice and the result substituted back to eliminate the integral term, there results

$$\frac{1}{4}\frac{\partial^3 T^+}{\partial z^2 \partial \tau} + \frac{\partial^2 T^+}{\partial z^2} - \frac{\partial T^+}{\partial \tau} = 0 \ . \tag{38}$$

If a Laplace transformation in τ is applied to this equation, it becomes

$$\frac{d^2\overline{T}^+}{dz^2}(p/4 + 1) - p\overline{T}^+ = 0 \ , \tag{39}$$

where $\overline{T}^+$ is the Laplace transform of T^+. The solution of this equation can be written

$$\overline{T}^+(z,p) = A_1 e^{r_1 z} + A_2 e^{r_2 z} \tag{40}$$

where

$$r_{1,2} = \pm [4p/(p + 4)]^{1/2} \ . \tag{41}$$

The integration constants, A_1 and A_2, are determined by requiring that the solution, eqn. (40) satisfies the Laplace transformation of eqn. (37). The result is

$$A_1 = \frac{b_1 a_{22} - b_2 a_{12}}{a_{11} a_{22} - a_{12} a_{21}}$$

and (42)

$$A_2 = \frac{b_2 a_{11} - b_1 a_{21}}{a_{11} a_{22} - a_{12} a_{21}}$$

where

$$a_{11} = (1 + p/4) - (e^{(r_1 - 2)\ell} - 1)/(r_1 - 2)$$

$$a_{12} = (1 + p/4) - (e^{(r_2 - 2)\ell} - 1)/(r_2 - 2)$$

$$a_{21} = e^{r_1 \ell}(1 + p/4) - e^{-2\ell}(e^{(r_1 + 2)\ell} - 1)/(r_1 + 2)$$

$$a_{22} = e^{r_2 \ell}(1 + p/4) - e^{-2\ell}(e^{(r_2 + 2)\ell} - 1)/(r_2 + 2)$$

$$b_1 = e^{-2\ell}(1 - T_o^{*4})/8p$$

$$b_2 = (1 - T_o^{*4})/8p$$

By use of the inversion integral, the solution for $T^+(z,\tau)$ can be written

$$T^+(z,\tau) = \frac{1}{2\pi i}\left\{\int_\Gamma A_1 \exp(p\tau + r_1 z)\, dp + \int_\Gamma A_2 \exp(p\tau + r_2 z)\, dp\right\}, \tag{43}$$

where Γ is the path to the right of all singularities such that the real part of p is equal to a constant. A complete analytic solution does not appear possible, but asymptotic solutions for $\tau << 1$ and $\tau >> 1$ can be found.

4.2.1 Short-time solution

Large p corresponds to small τ; thus

$$r_{1,2} = \pm 2(1 - 2/p),$$

$$A_1 = e^{-2\ell}(1 - T_o^{*4})\,[1 + (4\ell - 3)/p]/2p^2$$

$$A_2 = -e^{-2\ell}(1 - T_o^{*4})[1 - 2(3 - 2\ell)/p]/2p^3$$

whence

$$T^+(z,\tau) = (1/2)e^{-2(\ell - z)}(1 - T_o^{*4})\left\{1 + \left[\frac{4\ell - 3}{2} - 2\left(z + \frac{e^{-4z}}{4}\right)\right]\tau\right\}\tau + O(\tau^3) \tag{44}$$

and, following previous usage,

$$T(z,\tau) = T_i[1 - 4T^+(z,\tau)]^{1/4} \quad . \tag{45}$$

4.2.2 Long-time solution

For large τ, the form of the integrals in the inversion equation suggests that the dominant contribution comes from the neighborhood of the stationary (saddle) point enclosed by the contour path is located near the origin. Thus r_1, r_2, A_1 and A_2 can be approximated adequately by expanding these functions for small p [10]. When this is done, the transformed temperature distribution becomes

$$\overline{T}^+(z,p) = \frac{1 + 2z}{8(1 + \ell)} \frac{(1 - T_o^{*4})}{p(1 + pM)} \tag{46}$$

whence

$$T^+(z,\tau) = \frac{1 + 2z}{8(1 + \ell)} (1 - T_o^{*4}) [1-\exp(-\tau/M)] \tag{47}$$

where

$$M = \frac{\frac{(1-e^{-2\ell}) + 5\ell/2}{2(1-e^{-4\ell})} + \frac{\ell}{4}}{1 + \ell} \quad . \tag{48}$$

As $\tau \to \infty$, eqn. (47) provides exactly the steady-state distribution obtained previously.

Sample results are shown in Figure 9 for T/T_i at the mid-position of the cylinder (at $z = \ell/2$) as a function of τ for various values of T_o^* but with $\ell = 1$ for all cases. Figure 10 illustrates the effect of different ℓ with $T_o^* = 0$.

For large values of L compared with the radiation mean free path (say $\ell > 2$), the accuracy of these asymptotic approximations can be

improved by taking terms of higher order of smallness into consideration. It is also possible to obtain transient solutions appropriate for semi-infinite cylinder length, as described next.

4.2.3 The semi-infinite cylindrical geometry

In the previous work the origin of the coordinate system has been taken on the edge of the plates (or at the end of the cylinder) where the radiation boundary conditions remained constant at all times. When a semi-infinite geometry is considered the cylindrical tube has only one end, so to speak, and it is from that end that transients must be induced and also any coordinate system must begin. Accordingly, attention is given here to the case $\ell \to \infty$, with the initial and boundary conditions:

$$\begin{aligned} T &= T_i \quad \text{for} \quad \tau = 0 \\ T &= T_o \quad \text{for} \quad x = 0^-, \quad \tau > 0 \ . \end{aligned} \tag{49}$$

The analysis of this case follows that for the finite length tube, through the first Laplace transformation to the solution of the form

$$\bar{T}^+ (z,p) = A_1 e^{r_1 z} + A_2 e^{r_2 z} \tag{50}$$

with

$$r_{1,2} = \pm [4p/(P + 4)]^{1/2}$$

but since T^+ is finite, A_1 is zero. A_2 can then be found once T_o has been selected. For simplicity in illustration, it is assumed here that $T_o = 0$. Then

$$A_2 = A = 1/8p \ (1 - 1/(r + 2) + p/4) \ .$$

Again, it is possible to obtain short-time and long-time approximations:

(i) For short times, i.e. $p \gg 1$,

$$r \sim 2(1 - 2/p)$$

$$A \sim (1/2p^2) - (3/2p^3)$$

when these values are substituted and the inverse Laplace transform is taken

$$T^+(z,\tau) = e^{-2z}[(\tau/16z)^{1/2} I_1(4\sqrt{z\tau}) - (3\tau/8z) I_2(4\sqrt{z\tau})] \ .$$

The modified Bessel function has an asymptotic form for $x_j \to 0$:

$$I_\nu(x_j) \sim (x_j/2)^\nu / \Gamma(\nu+1) \ ,$$

provided that ν is a non-negative integer, whence

$$T^+(z,\tau) = \frac{1}{2} e^{-2z} (\tau - 3\tau^2/2) \qquad (51)$$

with

$$T(z,\tau) = T_i[1 - 4T^+(z,\tau)]^{1/4}$$

as usual.

(ii) For long times,

$$r \sim p^{1/2} - 0 (p^{3/2})$$

$$A \sim 1/4p - 1/8p^{1/2}$$

whence

$$T^+(z,\tau) = \frac{1}{4} \operatorname{erfc} \frac{z}{2\tau^{1/2}} - \frac{1}{8(\pi\tau)^{1/2}} \exp(-z^2/4\tau) \qquad (52)$$

It is interesting that this long-time solution contains a term which

corresponds to the transient pure conduction solution for corresponding boundary conditions. The argument of the complementary error function here can be compared with that for pure conduction; the quantity which replaces the conductive diffusivity is $(\sigma T_i^3 D^2/\delta\rho c)$, and this is the radiation diffusivity adduced previously. Here, it is seen to arise naturally in the solution of a problem where the geometry is optically thick.

4.3 The hollow cylinder with distributed heat sources

In Section 3.2 the steady-state temperature distribution for this configuration was discussed. Here, it is intended to seek a solution for a typical transient condition. From the steady-state solution, for $q(z) = Q$,

$$T(0) = T_i[c_1 + (Q/\sigma T_i^4)(1 + \ell)]^{1/4} .$$

It is more convenient to non-dimensionalize temperatures and time using $T(0) = T_w$, than to use T_i as previously. If conduction is ignored, the local energy balance becomes

$$T^{*4}(z,\tau) = T_i^{*4} F(z) + \int_0^{\ell} T^{*4}(\xi,\tau) K(|z-\xi|) d\xi - \frac{\partial T^*(z,\tau)}{\partial \tau} . \qquad (53)$$

The initial and boundary conditions are that for

$$\begin{aligned} &\tau = 0, \quad T^*(x) \text{ is the steady-state distribution with } Q = \text{constant} \\ &\tau > 0, \quad T = T_i \text{ at } z = 0^-, \quad Q = 0, \\ &\qquad \text{and } T = 0 \text{ at } z = \ell^+ . \end{aligned} \qquad (54)$$

The technique used previously for the cylindrical geometry can be employed again. T^* is linearized, which places restriction on the

combination of Q/T_i^4 and ℓ which can be considered; indeed, it is convenient to assume

$$C_2 - (2Q/\sigma T_i^4)\,\ell \ll C_1 + (Q/\sigma T_i^4)(1 + \ell) ,$$

where C_1 and C_2 are constants from the steadystate solution, since this makes T^+ directly proportional to x. Twice-repeated differentiation and substitution dispose of the integral and give exactly the same equation as eqn. (38) in Section 4.2, except that here the variables have different non-dimensionlization. If a Laplace transformation in τ is applied, the resulting equation is

$$\frac{d^2\overline{T}^+}{dz^2}(p/4+1) - p\overline{T}^+ = \frac{1}{4}\frac{d^2T^+(z,0)}{dx^2} - T^+(z,0) = a_1(1 + b_1 z - 2z^2) \tag{55}$$

where

$$a_1 = (Q/4\sigma T_i^4)/[c_1 + (Q/\sigma T_i^4)(1 + \ell)]$$

and

$$b_1 = 2\ell - c_2\sigma T_i^4/Q .$$

The complementary solution is given by

$$\overline{T}_c^+ = B_1 e^{r_1 z} + B_2 e^{r_2 z} \tag{56a}$$

with

$$r_{1,2} = \pm [4p/(p + 4)]^{1/2} ,$$

and the particular solution by

$$\overline{T}_p^+ = 2a_1 z^2/p - a_1 b_1 z/p + 4a_1/p^2 \ , \qquad (56b)$$

so that

$$\overline{T}^+ = \overline{T}_c^+ + \overline{T}_p^+ \ .$$

Since a finite tube is considered (i.e. B_1 is not eliminated), it is possible to find B_1 and B_2 by taking the Laplace transform of the linearized integral equation and substituting $z = 0$ and $z = \ell$. Again, no complete inversion can be found, but the short-time approximation ($p >> 1$) comes out to be

$$T^+(z,\tau) = (2a_1 z^2 - a_1 b_1 z) + \left\{ \frac{4[f(\ell)e^{2z} + g(\ell)e^{-2z}]}{e^{2\ell} + e^{-2\ell}} + 4a_1 \right\} \tau \qquad (57)$$

where

$$f(\ell) = F(\ell)\, e^{-2\ell} - G(\ell)$$

$$g(\ell) = G(\ell) - F(\ell)\, e^{2\ell}$$

$$F(\ell) = (1 - T_i^{*4})/8 + e^{-2\ell}/8 - a_1 - a_1(e^{-2\ell}(\ell^2+\ell) - 1/2) + (a_1 b_1/4)\,(e^{-2\ell}(2\ell+1) - 1)$$

$$G(\ell) = (1/8)\,(e^{-2\ell}(1 - T_i^{*4}) + 1) - a_1 - (2a_1\ell^2 - a_1 b_1 \ell) + e^{-2\ell}\{a_1[e^{2\ell}(\ell^2 - \ell + 1/2) - 1/2] - (a_1 b_1/4)[e^{2\ell}(2\ell - 1) + 1]\}$$

and

$$T(z,\tau) = T_w[1 - 4T^+(z,\tau)]^{1/4} \ .$$

The first term in the short-time transient solution, eqn. (57), is simply the steady-state solution, as expected.

4.4 Accounting for transverse temperature variation in the wall

When the parameter

$$\frac{\sigma T_i^3 a^2}{\delta k} \left(\frac{\delta^2}{L^2}\right)$$

is smaller than unity, but not by a very large factor, it is necessary to make an accounting for transverse temperature variation in the wall. If $(L^2/\delta^2) >> 1$, this accounting for transient wall conduction is important only for short times. It is a characteristic of short-time solutions that the linearized wall temperature perturbation, T^+, changes linearly with τ. The solution of the transient conduction problem in a wall of finite thickness with a constant heat flux applied at each surface, or with a surface temperature which changes linearly with time, is quite simple. For times smaller than the wall penetration time, the temperature distribution is very close to that in a semi-infinite slab subjected to the same boundary conditions; for larger times, the wall transverse temperature distribution is parabolic, with the average temperature through the wall different from the wall surface temperature by $(1/6\alpha\delta)\,(\partial T/\partial t)$, and the latter case is only a minor modification of the cases discussed above. For times smaller than the wall penetration time, however, the effective heat capacity of the walls depends upon the penetration depth, which is a function of time. As a consequence of this, the radiation diffusivity is itself a function of time, and the wall temperature does not change linearly with time, even at short times.

In order to treat this problem simply, but without destroying essential features, an approximation method is used here to represent the transient transverse conduction. It is convenient to use a parabolic

profile approximation for the region of the penetration depth (cf. Lardner [11]). If y is the coordinate normal to the wall surface and with its origin on it, the temperature distribution may be taken as

$$T(z,y,t) = T_i - [T_i - T(z,0,\tau)](1 - y/\gamma)^2 \ . \qquad (58)$$

It is obvious that γ is the penetration depth in the wall, and this is known to vary as the square-root of time from initiation of the transient. Eqn. (58) has been written for the initial condition that $T = T_i$ everywhere. The mean temperature within the section of wall which has been passed by the transient front (i.e. the section from $y = 0$ to $y = \gamma$) is

$$\begin{aligned} T_m(z,t) &= (1/\gamma) \int_0^{\gamma} T(z,y,t)\, dy \\ &= (T_i/3)\, [2 + T^*(z,0,t)] \end{aligned}$$

so that

$$T_m^+(z,t) = (1/3)\, T^+(z,0,t) \ . \qquad (59)$$

The term which represents the internal energy change in the local energy balance equation becomes

$$\begin{aligned} -\frac{\partial}{\partial t} \frac{\gamma \rho c}{4\sigma T_i^3} T_m^+(z,t) &= -\frac{\rho c}{4\sigma T_i^3} \frac{\partial}{\partial t} [\gamma\, T_m^+(z,t)] \\ &= -\frac{\rho c}{12\sigma T_i^3} \frac{\partial}{\partial t} [\gamma\, T^+(z,0,t)] \qquad (60) \\ &= -\frac{1}{4} \frac{\partial T^+(z,0,\eta)}{\partial \eta} \end{aligned}$$

where

$$\eta = \frac{3\sigma T_i^3}{j(k\rho c)^{1/2}}\, t^{1/2}$$

with

$$\gamma = j(\alpha t)^{1/2} .$$

This solution is based on the approximation that the penetration depth increases as $t^{1/2}$, no matter how the surface temperature may be changing as a (monotonic) function of time, and on the assumption that the mean temperature within this depth can be regarded as a constant proportion of the surface temperature. It is no longer necessary that T^+ varies linearly with time. With this transformation, the local energy balance equation for the plate geometry is the same as eqn. (31) and for the cylindrical geometry becomes identical with eqn. (37), except that η replaces τ. The initial and boundary conditions considered here are the same as in Sections 4.1 and 4.2. Consequently, all the solutions obtained previously in Sections 4.1 and 4.2 can be applied, except that τ is replaced by η, so that the solutions differ when expressed in terms of t. A further feature of the solutions is that the z-dependence of T^+ is exactly the same whether η or τ is the dimensionless time variable; thus, if γ becomes equal to δ at some finite η, the solution can be switched over to the expressions for $T^+(z,\tau)$ but with use of a matching time variable, τ', defined by

$$T^+(z,0,\eta) = T^+(z,\tau') \quad \text{when} \quad \gamma = \delta . \tag{61}$$

This technique should be satisfactory when τ' falls within the range of values appropriate to a short-time solution.

If $\delta \not< a$ (or D), the energy balance must be modified to include the energy flux at the solid surfaces in the planes $x = 0$, $x = L$. This can be readily accomplished in a variational formulation

for the problem, or in a numerical scheme (such as used by Winter [5]). It is more difficult to incorporate it into the scheme used previously in this section, because it destroys the one-dimensional treatment of transient conduction in the walls. A proposal for rapid treatment of this case is given in the Discussion.

As an illustration of a solution involving use of η, a comparison has been made with Winter's results. To make this comparison, the solution for short times (Section 4.1.1) has been used, with ν small enough that the radiation "penetration depth" has not reached $z = 1$. The comparison cannot be expected to be good near the open end of the slots, because the analysis here takes no account of the end-surface heat transfer. However, at very short times the penetration depth is only a very small fraction of the slab half-width for Winter's parameters; for example, Winter's (dimensionless) time t for half-thickness penetration is about 0.8 for $s = 5$ and about 3 for $s = 10$. The short-time solution was compared with Winter's solutions for $w = 2$, $s = 5$ with $t = 0.01$, and for $w = 1$, $s = 10$ with $t = 0.002$, 0.006 and 0.01. (A computer output tabulation was kindly provided by Dr. Winter for $w = 1$ and $s = 10$, and this permitted close comparison.) The results were very close indeed to the analysis here, departing in the region of small y, i.e. in the region of z close to unity, due to the different boundary conditions applied to the end plane $y = 0$ $(z = 1)$ in the two cases. The difference between the solutions is presented in terms of their respective differences from the initial temperature, T_i, in Fig. 11. The magnitude of the difference between the solutions is divided by $(1 - T/T_i)$. For Winter's $t = 0.006$ and 0.01 the magnitude of this difference is of the order of 5 per cent;

for $t = 0.002$ it is about 27 per cent. This larger difference may be due to the difficulties in obtaining an adequate numerical solution after only one time-increment in Winter's solution. Even with this, the error in T/T_i is extremely small and the comparison between the solutions must be considered very satisfactory.

Transverse conduction in the wall of a hollow cylinder (or hole in a solid) can be treated in a similar manner, particularly if the penetration depth is not large compared with the hole radius over the time interval of interest. Even when this latter condition is not satisfied it is still possible to perform an analysis, but the details are more cumbersome.

5. SUPERPOSITION

It is natural to examine the practical feasibility of superposition of the results obtained in the previous section for analysis of problems with continuously varying boundary conditions. The analysis of transient solutions (above) involved linearization, and the results exhibited a diffusion effect rather clearly, with a radiation diffusivity which is distinct from the molecular diffusivity.

Superposition of solutions for T is possible with some similarity to the methods and results for ordinary conduction in a solid, but with some difference as well. It is well known that for ordinary conduction in a semi-infinite slab with a harmonically oscillating boundary temperature of frequency ω the solution posses a characteristic diffusion length, $\gamma' = (2\alpha/\omega)^{1/2}$. If the radiation diffusivity is substituted for α, a characteristic radiation diffusion length Λ is obtained, e.g. for a hollow cylinder

$$\Lambda = \left(\frac{2\sigma T_i^3 D^2}{\delta \rho c \omega}\right)^{1/2} \tag{62}$$

If the wall has a small thermal diffusivity, δ can be replaced by $(2\alpha/\omega)^{1/2}$ for the wall. It is obvious that Λ can be large or small compared with the radiation mean free path, depending upon whether ω is small or large. In the latter case no significant variation of wall temperature occurs beyond the order of one radiation mean free path into the slot or hole, but it always occurs to that depth because the dominant cause of wall surface temperature change at short times is direct exchange with the outside environment. The attenuation of temperature change which occurs with increasing z in the short-time solutions, eqns. (34) and (44), is due entirely to the reduction of the

view factor of the environment with increasing z.

There are convenient non-dimensional forms for ω, corresponding to the transformations for τ and η used in the previous sections; for thin walls,

$$\Omega = \frac{\omega \delta \rho c}{\sigma T_i^3} \tag{63}$$

and for thick walls

$$\Xi = \frac{k\sqrt{2}}{\sigma T_i^3 \gamma'} \tag{64}$$

The cases $\Omega \to 0$, $\Xi \to 0$ correspond to the radiation mean free path being much smaller than the radiation diffusion length, Λ.

5.1 High-frequency oscillations

Two methods can be applied to obtain solutions for high frequency oscillations. The first method is to consider each section of the wall (at different z) as autonomous, to determine the local "heat transfer coefficient" for linearized radiation, and then apply the results to the solutions described by Carslaw and Jaeger [12]. The periodic boundary condition can be specified as $T_o(z = 1^+, t) = T_i - T_a \cos\omega t$. Solution for $\Omega \to \infty$, $t \to \infty$ gives a result where $4T_a^{*}/\Omega$ replaces $(1 - T_o^{*4})$ in the short-time solution, eqn. (34), and $\cos(\omega t - \pi/2)$ replaces τ. A similar result is obtained for $\Xi \to \infty$ except that the wall surface phase lag in temperature is reduced from $\pi/2$ to $\pi/4$.

The second method is to use superposition directly with the solutions obtained in the previous section. Duhamel's theorem can be written for a region bounded by two planes:

$$v(x,t) = \int_0^t [\chi_1(\lambda) \frac{\partial}{\partial t} F_1(x,t - \lambda) + \chi_2(\lambda) \frac{\partial}{\partial t} F_2(x,t - \lambda)] \, d\lambda$$

and for the parallel-plane example the functions can be taken as

$$\chi_1(\tau) = 0, \quad \chi_2(\tau) = T_a^* \cos\Omega\tau$$

and

$$F_2(z,\tau) = (1/2) \left\{1 - \frac{1 - z}{[\nu^2 + (1 - z)^2]^{1/2}}\right\} \tau$$

which lead, by substitution and integration, to

$$T^+(z,\tau) = (T_a^*/2\Omega) \left\{1 - \frac{1 - z}{[\nu^2 + (1 - z)^2]^{1/2}}\right\} \cos(\Omega\tau - \pi/2) \qquad (65)$$

in agreement with the result for thin walls from the first method. For the thick-walled case, a solution can also be obtained; it is convenient for this to retain the definitions of both τ and η. Thus $\Xi^2\tau = \omega t$. By Duhamel's theorem and the short-time solution, eqn. (34),

$$T^+(z,\tau) = \int_0^\tau T_a^* \cos(\Xi^2\lambda) \frac{\partial}{\partial\tau} \left\{\frac{1}{2}\left[1 - \frac{1 - z}{[\nu^2 + (1 - z)^2]^{1/2}}\right] \frac{3}{j} (\tau-\lambda)^{1/2}\right\} d\lambda \qquad (66)$$

The τ-dependent term in this equation is

$$\int_0^\tau \frac{\cos\Xi^2\lambda}{(\tau - \lambda)^{1/2}} \, d\lambda \, .$$

This can be reduced by the substitution $\tau - \lambda = u$, separation of τ and u by use of a trigonometric identity; substitution of $v = \Xi^2 u$ then gives the τ-dependent factor as

$$\frac{1}{\Xi} \left\{\cos(\Xi^2\tau) \int_0^{\Xi^2\tau} \frac{\cos v}{v^{1/2}} \, dv + \sin(\Xi^2\tau) \int_0^{\Xi^2\tau} \frac{\sin v}{v^{1/2}} \, dv \right\} .$$

The integrals can be recognized as Fresnel integrals, so that the temperature distribution is

$$T^+(z,\tau) = \frac{3(2\pi)^{1/2}}{4\,j}\,\frac{T_a^*}{\Xi}\left\{1 - \frac{1-z}{[\nu^2 + (1-z)^2]^{1/2}}\right\} x$$

$$x\,[\cos(\Xi^2\tau)C_2(\Xi^2\tau) + \sin(\Xi^2\tau)S_2(\Xi^2\tau)]\ . \qquad (67)$$

When $\tau \neq 0$ and $\Xi \to \infty$, the time-dependent factor (in brackets in eqn. (67)) becomes

$$(1/\sqrt{2})\,\cos\,(\Xi^2\tau - \pi/4)\ .$$

When this is substituted in eqn. (67) the result corresponds to the solution obtained for the wall surface by the first method, if the exact value for j for the transient wall conduction is used. The results obtained by the second method, i.e. by direct superposition of the solutions in Section 4, involved use only of short-time solutions even though λ progresses to values of τ which were not small. While this is intuitively reasonable, further justification can be found below.

5.2 Low-frequency solutions

Equation (36) is in fact the full-range transient solution for the parallel plate case; the leading term contracts to the short-time solution for small τ. With this solution it is therefore possible to apply Duhamel's theorem and to obtain a full-range solution for, say, $T_o = T_i - T_a \cos \Omega\tau$. This solution is

$$T^+(z,\tau) = \frac{T_a^*}{\Omega}\,\phi_o(z)\,\sin\Omega\tau - \frac{16T_a^*}{\Omega^2}\,\phi_1(z)\,(\cos\Omega\tau - e^{-4\tau}) - \ldots. \qquad (68)$$

When $\Omega \to \infty$ this reduces to eqn. (65) obtained previously with use of the short-time solution.

These examples serve to illustrate that superposition can be readily accomplished.

6. DISCUSSION

6.1 The photon mean free effective path

There are two generalizations of this concept which are particularly useful. The first concerns geometries other than parallel plates and circular cylinders; the second concerns non-black surfaces.

The (black) photon mean free effective path at x_{jo} and in direction x_j is defined as the integral of radiation intensity absorbed by elements dA_2 of surfaces at a displacement $(x_j - x_{jo})$ from an elementary area dA_1 at x_{jo} times $(x_j - x_{jo})$, and divided by the integral of radiation from the element at x_{jo} to all $x_j > x_{jo}$, i.e.

$$\lambda = \frac{\int_{A_2:\ x_j > x_{jo}} (x_j - x_{jo})\ \sigma\ T^4_{x_{jo}}\ F_{12}\ dA_2}{\int_{A_2:\ x_j > x_{jo}} \sigma T^4_{x_{jo}}\ F_{12}\ dA_2}$$

This can be regarded as the integral of distance $(x_j - x_{jo})$ weighted by the proportion of the radiation from an elementary area at x_{jo} which is absorbed at x_j. For the parallel flat plates and for the hollow cylinder with black surfaces this came out to be particularly simple. However, there is nothing in principle to prevent application of the concept to other well-defined geometries involving cavities, e.g. hexagonal tubes, loosely stacked mats of crossed cylindrical rods (fibrous insulation) and so on. The quantity λ is non-isotropic in general. In every case it is assumed that the geometrical pattern is continued for an infinite distance in order to calculate λ.

One advantage of the concept of λ is found in bodies where the radiation path length is much larger than λ. In the interior the

basic integro-differential equation can be approximated with good accuracy by a differential equation involving a weighted conductivity (radiation plus molecular conduction), and the solution for this matched to solutions for the "edges" of the body which can see the radiation environments fairly directly. The "edges" can be taken to extend about 2λ into the body from its external surfaces. This method of approximation can work well for steady-state and low-frequency oscillatory solutions, but for high-frequency oscillations or short-time transients the considerations in the previous sections apply again.

In order to understand how λ can be computed for non-black surfaces it is useful to revert to its interpretation as the integral of distance $(x_j - x_{jo})$ weighted by the proportion of the radiation from an elementary area at x_{jo} which is absorbed at x_j. For the non-black case some of the radiation incident at x_j is reflected. The subsequent distribution of unabsorbed radiation and its eventual absorption can be computed. The quantity λ is affected by whether reflection is computed for $x_j > x_{jo}$ only, or whether reflection is considered for all x_j, absorption being considered only in the region $x_j > x_{jo}$ in either case. The former case is appropriate for "edge" regions of a body, and the latter case for deep regions. With Lambertian surfaces, λ always increases as the reflectivity increases.

The increase in λ does not imply that the radiation conductivity is increased; for grey surfaces this latter quantity is

$$\varepsilon \sigma T_i^3 \lambda \tag{70}$$

and it varies roughly as $\varepsilon^{1/2}$ for $1 - \varepsilon << 1$. A corresponding radiation diffusivity can be defined. Use of the two grey λ's, the

grey radiation-conductivity and diffusivity as appropriate permit some of the solutions obtained in the previous sections to be applied to problems where $\varepsilon < 1$.

The fact that λ is controlled by both the geometry and emissivity of the surfaces can be used to advantage. For example, a multilayer insulation for cryogenic systems often consists of several thicknesses of polished foil. This gives excellent resistance to heat flow normal to the foil layers, but suffers from a high radiation conductivity along the layers if an end is exposed to a non-cryogenic heat source. The λ for this entering radiation can be greatly reduced by making the foil strongly wavy near the ends: it is best if the waviness varies from one layer to the next.

6.2 Treatment of transient radiation problems

Many problems of physical interest can be treated within the framework of the solutions presented in earlier sections, especially with the extensions of the concepts of photon mean free effective path, radiation conductivity and diffusivity outlined in Section 6.1. However, there are some situations for which these solutions are insufficient. For example, when the thickness of the solid sections of a slotted slab is not small compared with the slot widths, the transient conduction problem can be treated as approximately one-dimensional at neighboring faces only at very short times. The slots might not be normal to the end faces, but inclined through the slab (like a tilted venetian blind), or the slab sections might not have flat ends ... . In all such problems it is still possible to follow the general scheme for calculations described explicitly here (for two geometries), but

making some necessary adaptations. If the radiation diffusivity is large compared with the (molecular) thermal diffusivity, and the cavities are long compared with the radiation mean free path, the region where two-dimensional effects are significant in the solid extends only to about 3δ in the slot direction. For this length into the slot, or for 2 radiation mean free paths, whichever is greater, the transient in this edge region can be studied with the help of numerical methods and matched to an analytic solution for the deeper regions where the effects are more simply accounted for. This hybrid scheme has the advantage that it can considerably reduce the time consumed in numerical analysis in studies like that undertaken by Winter [5]. The authors have found that a numerical program based on the method of finite elements [13] is useful for this.

It is worthwhile to note that at the beginning of this investigation the authors had in mind the possibility of generating a variational principle for combined radiation and conduction which could be used to solve steady-state and transient problems in various geometries. It turned out that while this could be established, in use it was not as accurate (for a given level of computational effort) as the set of techniques described here.

6.3 The significance of linearization

Extensive use has been made here of a linearization of the radiation heat flux with respect to temperature. Linearization of one kind or another is frequently used in radiation analyses to make calculations tractable, but this often means that only a very approximate answer is obtained. At first sight, the use of a linearization for the problems discussed here seems reasonable in the light

of the solutions themselves; the temperatures obtained in the solutions do not differ substantially from T_i.[#] The worst case--the greatest deviation from T_i--seems to be in the steady-state solutions when L is many times the radiation mean free effective path, and even then only in the immediate vicinity of the cold end. It should be emphasized that the linearization employed here is in making the approximation

$$T^{*4} \approx 1 - 4T^{+}$$

and this relation is used both for substitution in the energy balance relation and in recovering the physical temperature after a solution in terms of T^{+} has been found, e.g. eqns. (26), (35), (45) and so on.

It is possible to demonstrate that this linearization technique gives excellent results. In particular, if this technique is applied to the energy balance equation for the hollow cylinder to obtain a steady-state solution, the result can be shown to be exactly the same as eqns. (9) and (10), Section 3.1. This is so for any L/R. For the parallel plates, a comparison of steady-state solutions for the energy balance equation with and without linearization, using variational techniques in both cases, shows that very small differences exist, e.g. for $\nu = 0.2$, $T_o = 0$, the difference at the cold end ($T^{*} = 0.61$) is only 5 per cent.

[#]Except for the hollow cylinder with heat generation along its walls, for which a different linearization is employed and certain restrictions are invoked: confer Section 4.3.

7. SUMMARY

1. Temperature distributions in a parallel-walled channel and in a hollow cylinder are considered, where each end of the channel or cylinder faces an environment of uniform but alterable temperature. The wall surfaces are assumed to be black.

2. The concept of mean free effective path for radiation in a channel is introduced.

3. A particular technique is used for linearizing the radiant heat flux in terms of temperature. Comparison with steady-state solutions which do not involve linearization is surprisingly good. This linearization is applied for some steady-state solutions and exclusively for transient solutions.

4. Steady-state solutions are obtained for both geometries with conduction in the walls omitted. Additionally, a solution for the parallel plates including the effect of longitudinal conduction is given.

5. Transient solutions valid for short and long times are obtained for a parallel-walled channel and a hollow cylinder having thin walls; in addition, a full-range solution is obtained for the channel, and a solution is found for a hollow cylinder of semi-infinite length. Some similarities to solutions for transient conduction are noted.

6. Steady-state and transient solutions are obtained for a hollow cylinder with heat generation at the wall.

7. Transient solutions are obtained for a parallel-walled channel and a hollow cylinder having (thermally) thick walls, so that transient conduction normal to wall surfaces is coupled into the problem.

8. It is demonstrated that computation can be carried out easily for problems which involve superposition of the transient solutions already obtained.

9. The concept of mean free effective path for radiation is generalized to non-black surfaces and to other geometries. The mean free effective path is significant to the determination of optical thickness in any geometry, and to the calculation of radiation conductivity and radiation diffusivity.

10. The use of the analytical results in conjunction with numerical solutions for restricted portions of other geometries is discussed.

ACKNOWLEDGEMENT

This work reported here was supported by the U.S. National Aeronautics and Space Administration under Grant NGR-40-002-012, and this support is gratefully acknowledged.

REFERENCES

1. E. M. Sparrow and A. Haji-Sheikh "A generalized variational method for calculating radiant interchange between surfaces" Trans. ASME, Jl. Heat Trans., vol. 87, pp. 103-109 (1965)

2. E. G. Keshock and R. Siegel "Combined radiation and convection in an asymmetrically heated parallel plate flow" Trans. ASME, Jl. Heat Trans., vol. 86, pp. 341-350 (1964)

3. R. Viskanta, Discussion on "Application of variational methods to radiation heat transfer calculations" Trans. ASME, Jl. Heat Trans., vol. 82, pp. 375-380 (1960)

4. C. M. Usiskin and R. Siegel "Thermal radiation from a cylindrical enclosure with specified wall heat flux" Trans. ASME, Jl. Heat Trans., vol. 82, pp. 369-374 (1960)

5. D. F. Winter "Transient radiative cooling of a semi-infinite solid with parallel-walled cavities" Int. Jl. Heat Mass Trans., vol. 9, pp. 527-532 (1966)

6. H. C. Hottel and J. D. Keller "Effect of radiation on heat transmission in furnaces and through openings" Trans. ASME, vol. 55, pp. 39-49 (1933)

7. H. Buckley "On the radiation from the inside of a circular cylinder" Phil. Mag., Seventh series: Part I, vol. 4, pp. 753-762 (1927); Part II, vol. 6, pp. 447-457 (1928)

8. R. F. Probstein "Radiation slip" AIAA Jl., vol. 1, pp. 1202-1204 (1963)

9. E. M. Sparrow "Radiation heat transfer between surfaces" Advances in Heat Transfer, vol. 2, pp. 399-452, Academic Press (1965)

10. W. Lick "Transient energy transfer by radiation and conduction" Int. Jl. Heat Mass Trans. vol. 8, pp. 119-127 (1965)

11. T. J. Lardner "Biot's variational principle in heat conduction" AIAA Jl., vol. 1, pp. 196-206 (1963)

12. H. S. Carslaw and J. C. Jaeger "Conduction of heat in solids" Clarendon Press, Oxford, 2nd edn. (1959)

13. E. L. Wilson "Structural analysis of axisymmetric solids" AIAA Jl., vol. 3, pp. 2269-2274 (1965)

FIGURE CAPTIONS

Figure 1. Geometries of configurations: (a) parallel-plate channel (b) hollow cylinder, radius R.

Figure 2. Steady temperature distribution in a hollow cylinder with one end facing an environment at $T = T_i$, the other end an environment at $T = 0$, for $\ell = 1, 2, 5$ and 10.

Figure 3. Total heat flux through a hollow cylinder as a function of ℓ. a represents the radiation which passes straight through without absorption; b is the radiation which is absorbed just once before passing out of the hollow cylinder; and c is the radiation which is absorbed and re-radiated at least twice before passing out of the hollow cylinder. The sum of these is the uppermost (solid) line.

Figure 4. Steady temperature distribution in a hollow cylinder with uniform heat flux along the wall with the ends facing environments at $T = T_i$ and $T = 0$ respectively.

Figure 5. Steady temperature distribution along parallel plates, with the ends facing environments at $T = T_i$ and $T = 0$ respectively.

Figure 6. Transient temperature distribution along parallel plates at short times.

Figure 7. Transient temperature at the mid-point of parallel plates for $\nu = 1$.

Figure 8. Transient temperature at the mid-point of parallel plates for $T_o = 0$.

Figure 9. Transient temperature at the mid-point of a hollow cylinder for $\ell = 1$.

Figure 10. Transient temperature at the mid-point of a hollow cylinder for $T_o = 0$.

Figure 11. Comparison of transient temperature distribution on the thick walls in a slot from analysis given here and Winter's numerical solution.

PDR:gk
4/24/67

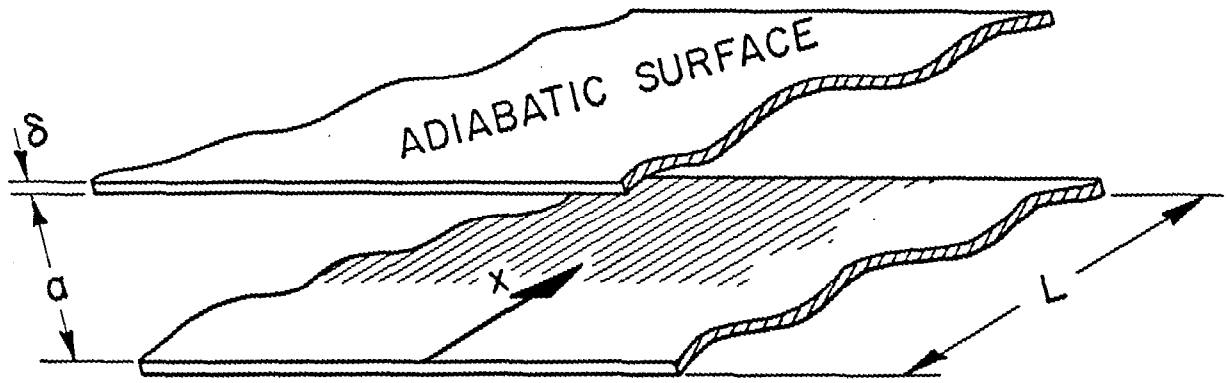

(a)

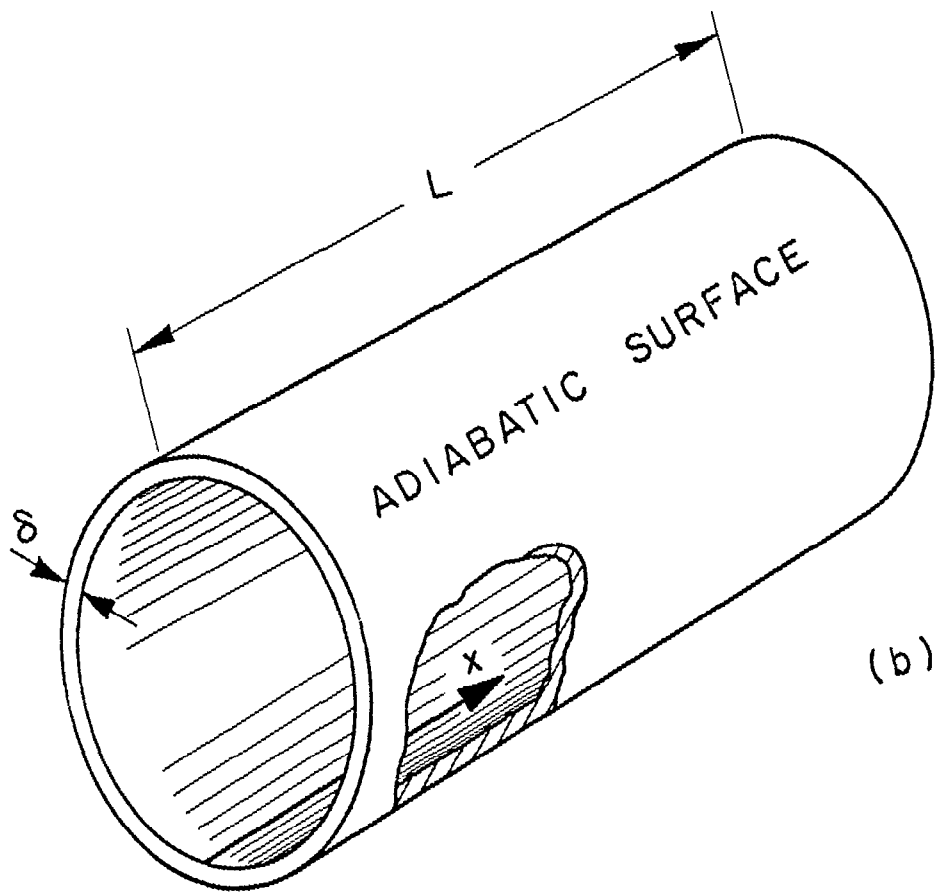

(b)

Figure 1

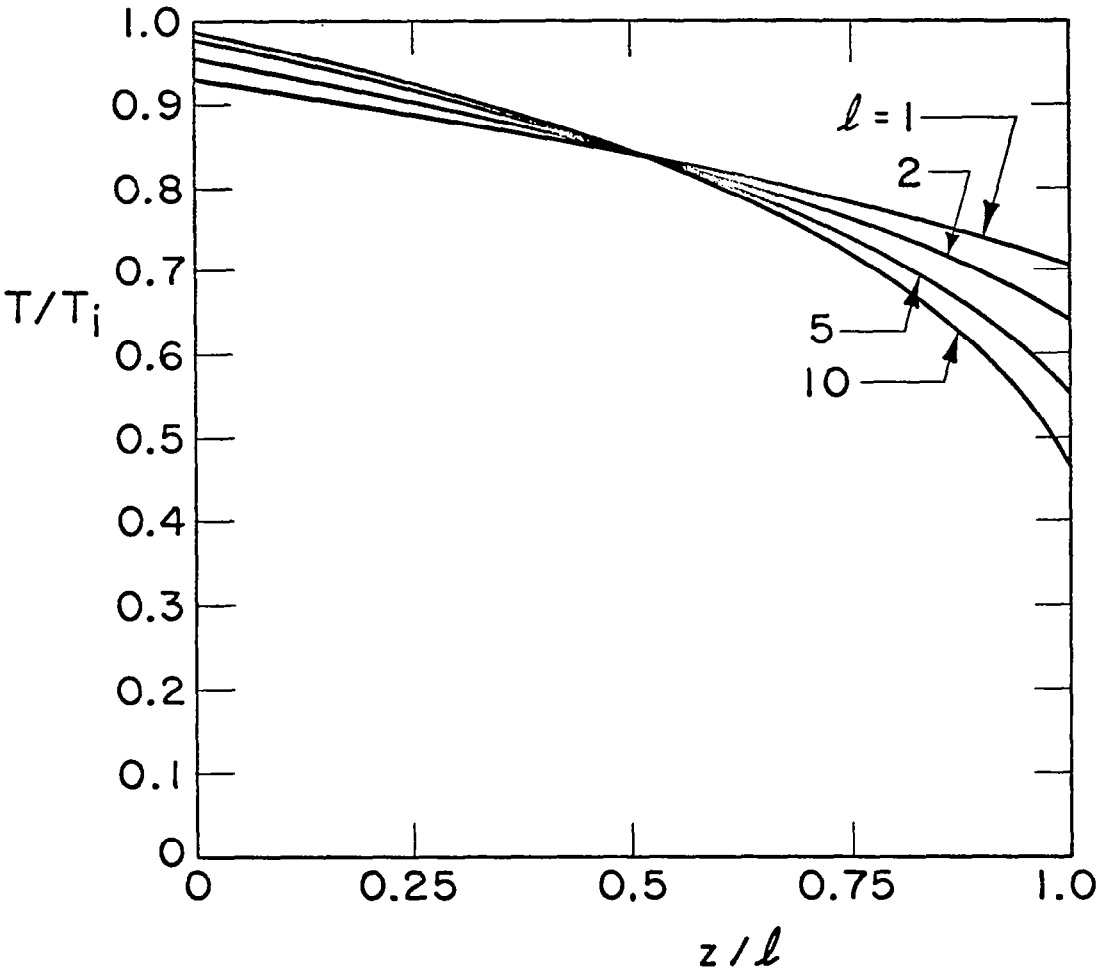

Figure 2

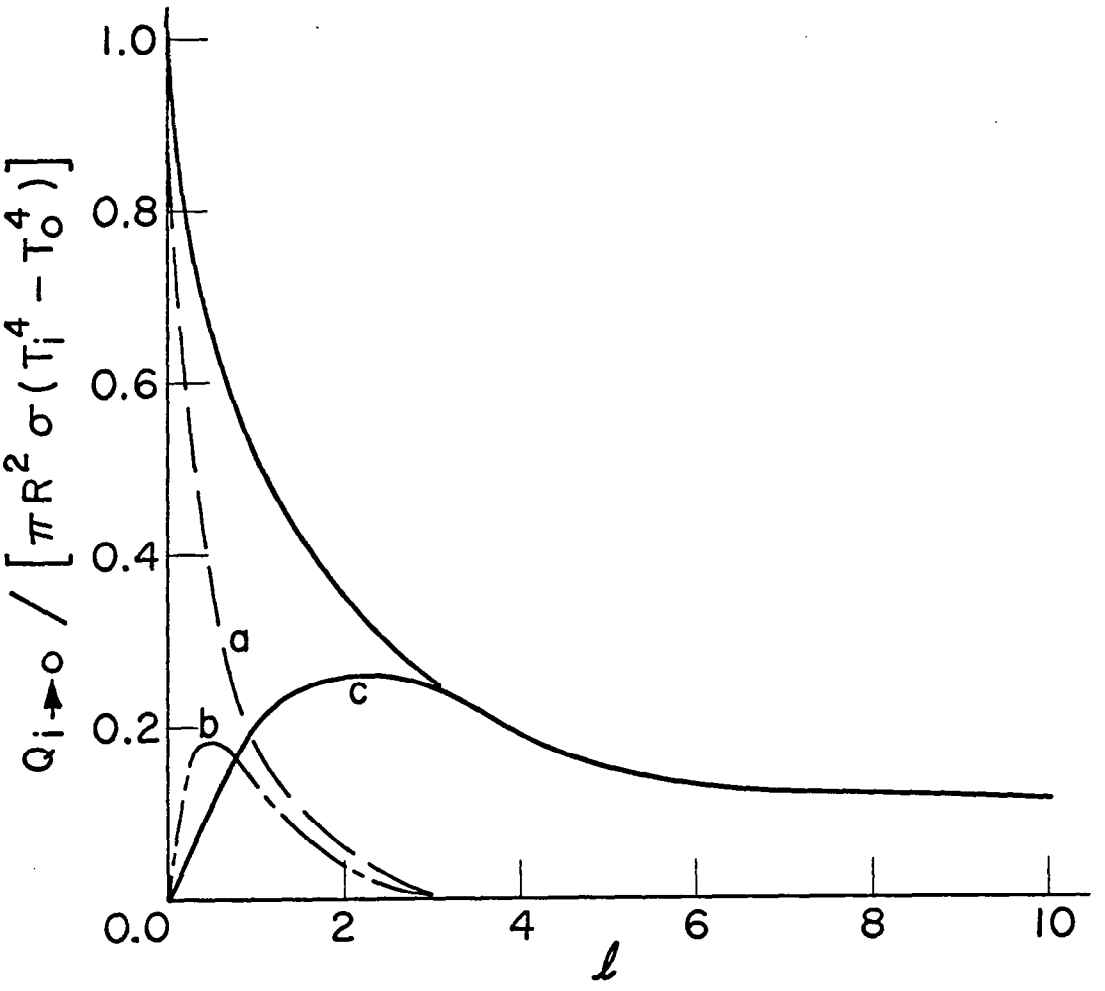

Figure 3

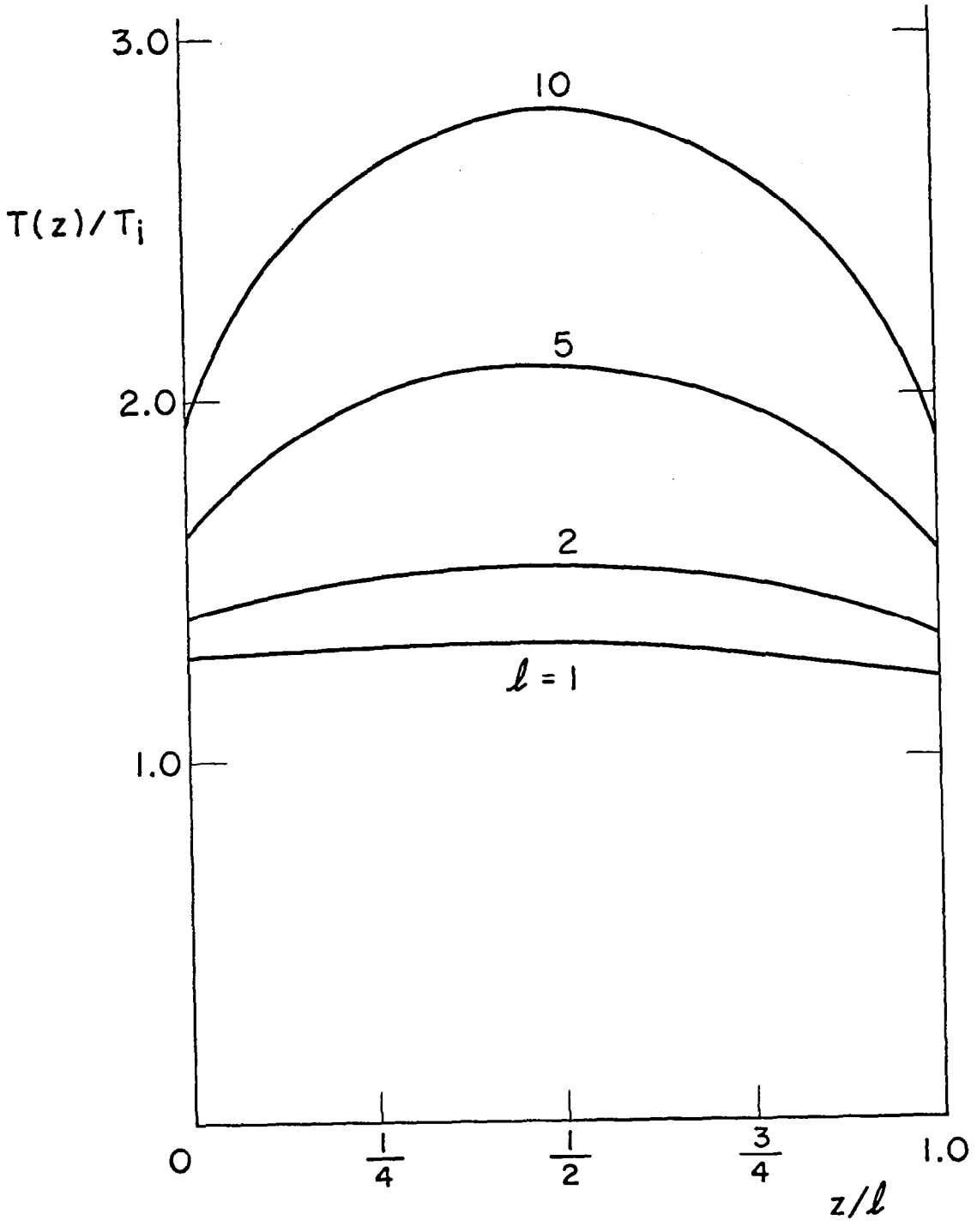

Figure 4

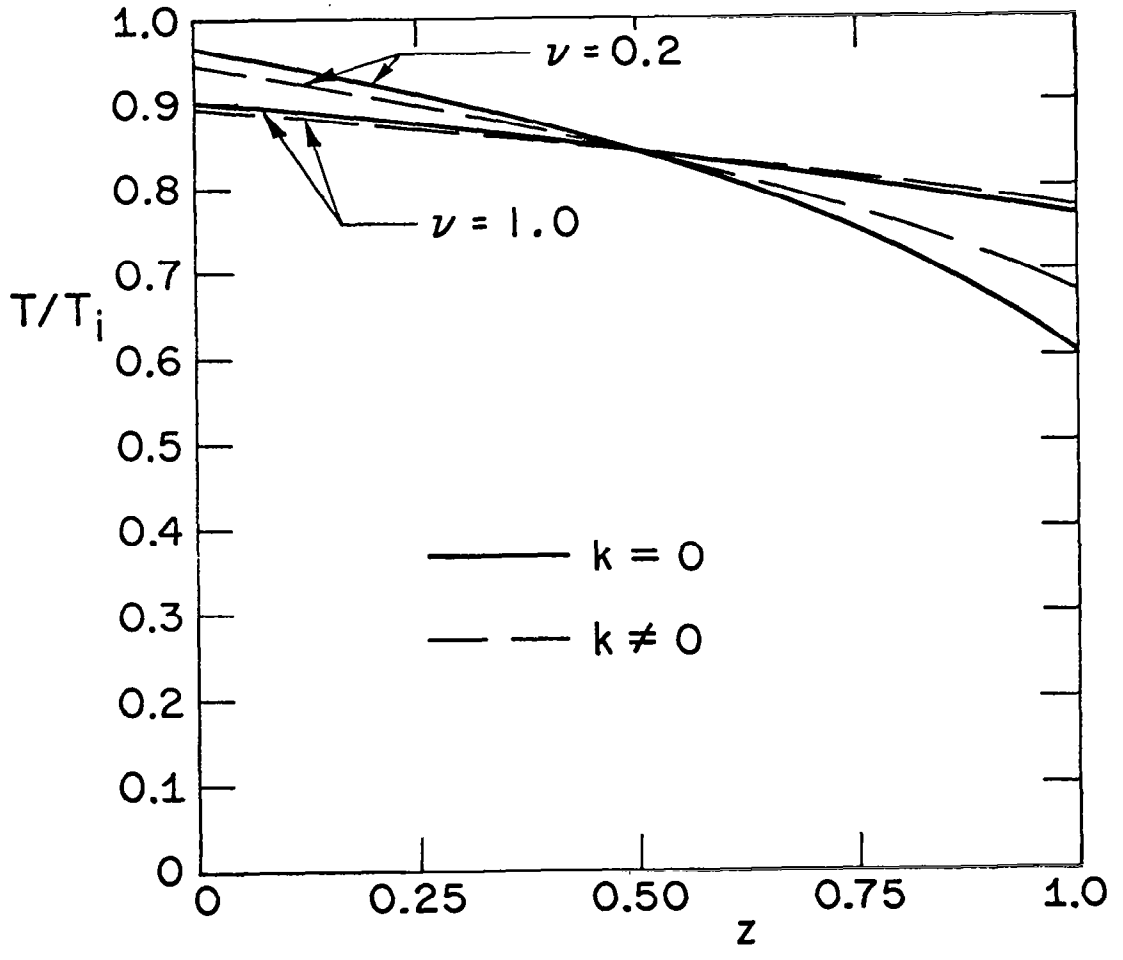

Figure 5

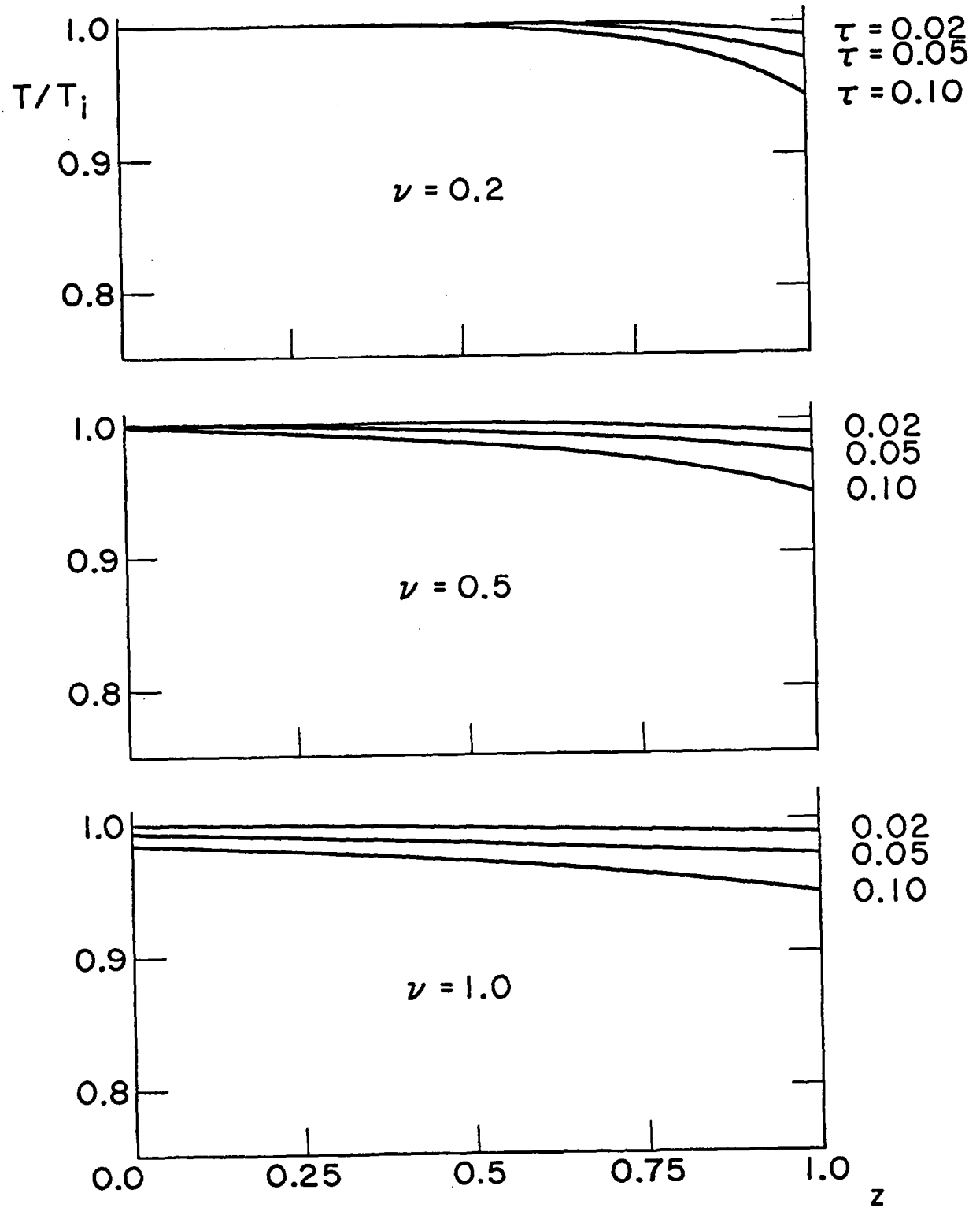
1.0
T/T_i
0.9
0.8
ν = 0.2
τ = 0.02
τ = 0.05
τ = 0.10
1.0
0.9
0.8
ν = 0.5
0.02
0.05
0.10
1.0
0.9
0.8
ν = 1.0
0.02
0.05
0.10
0.0
0.25
0.5
0.75
1.0
z

Figure 6

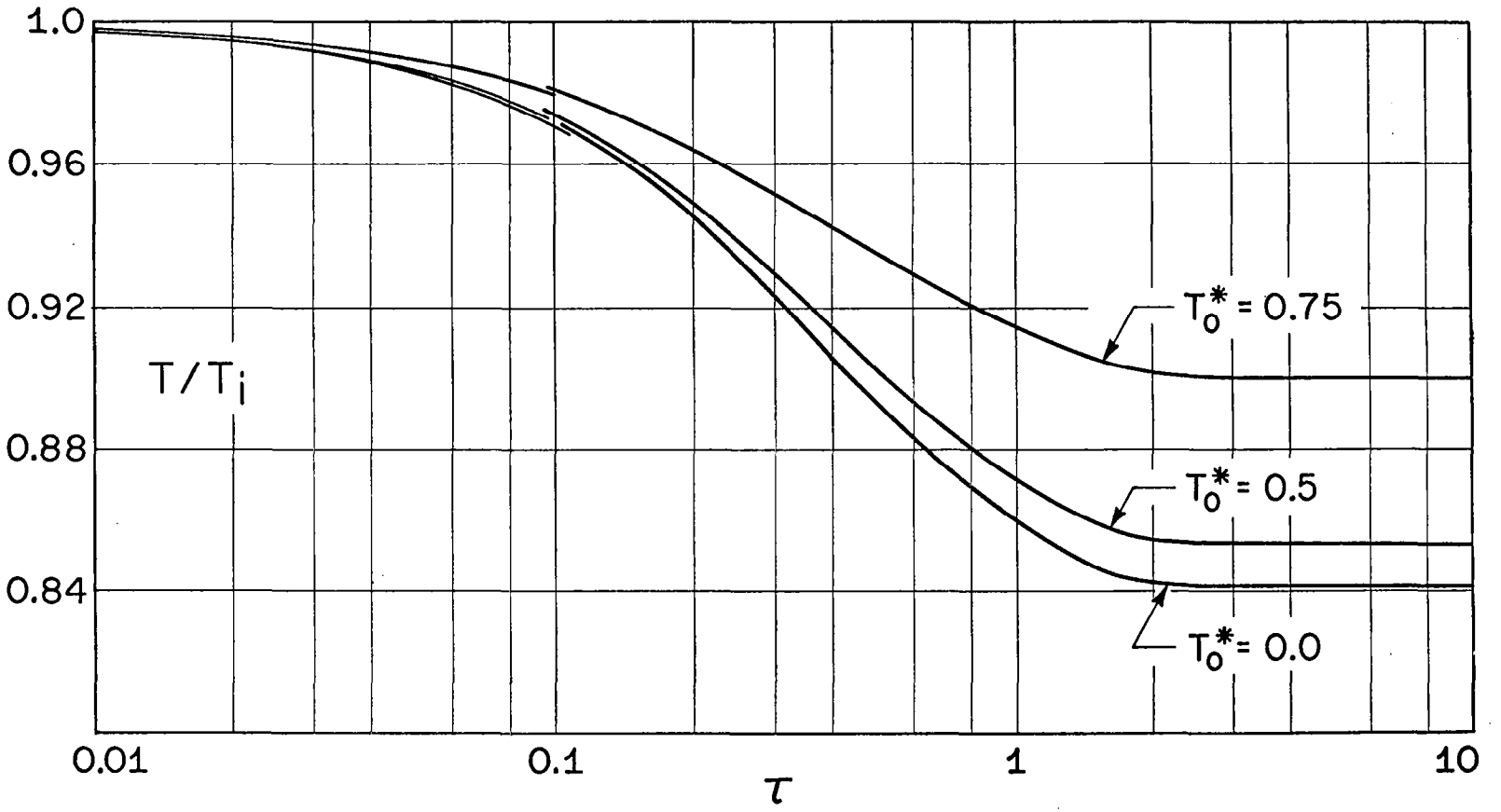

Figure 7

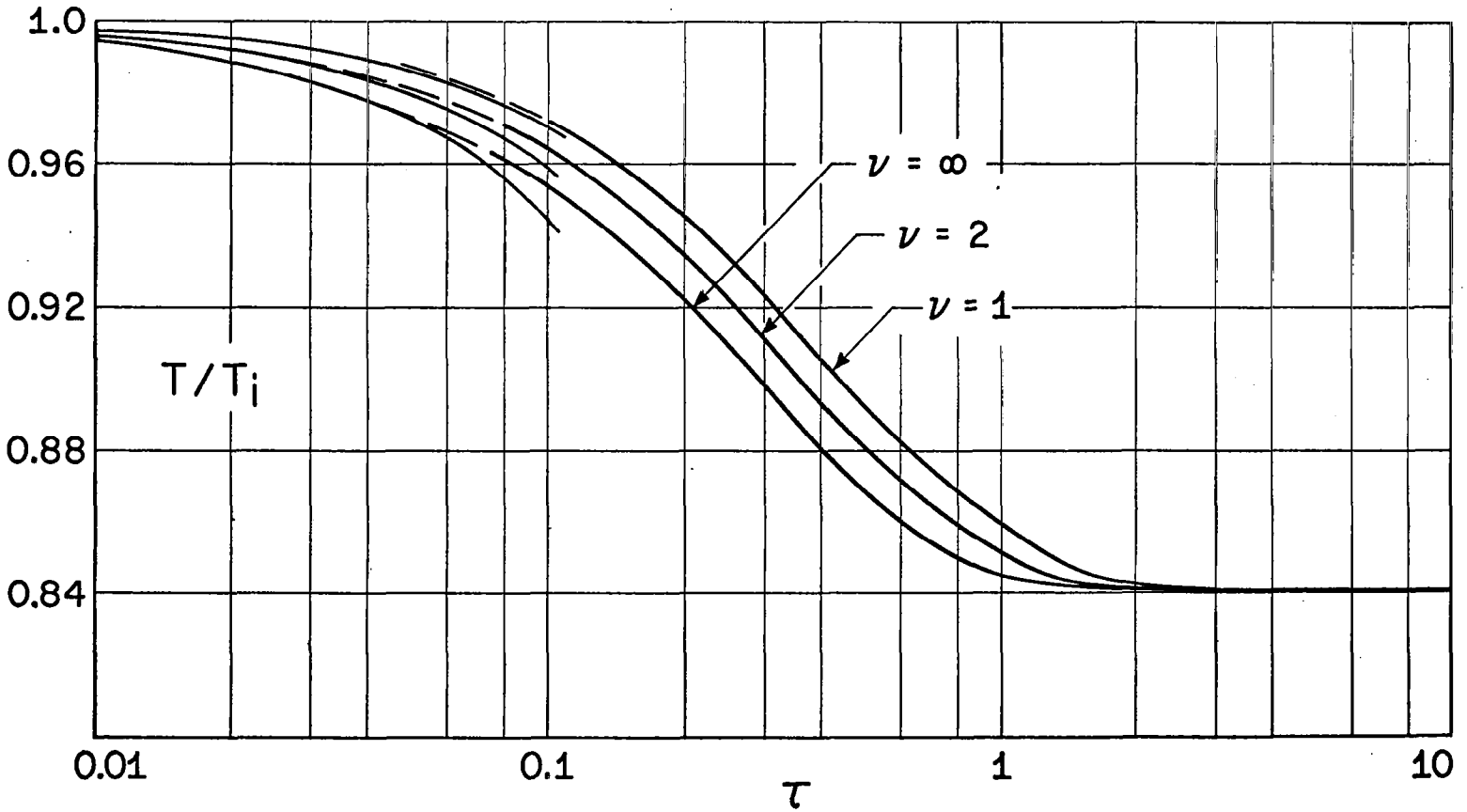

Figure 8

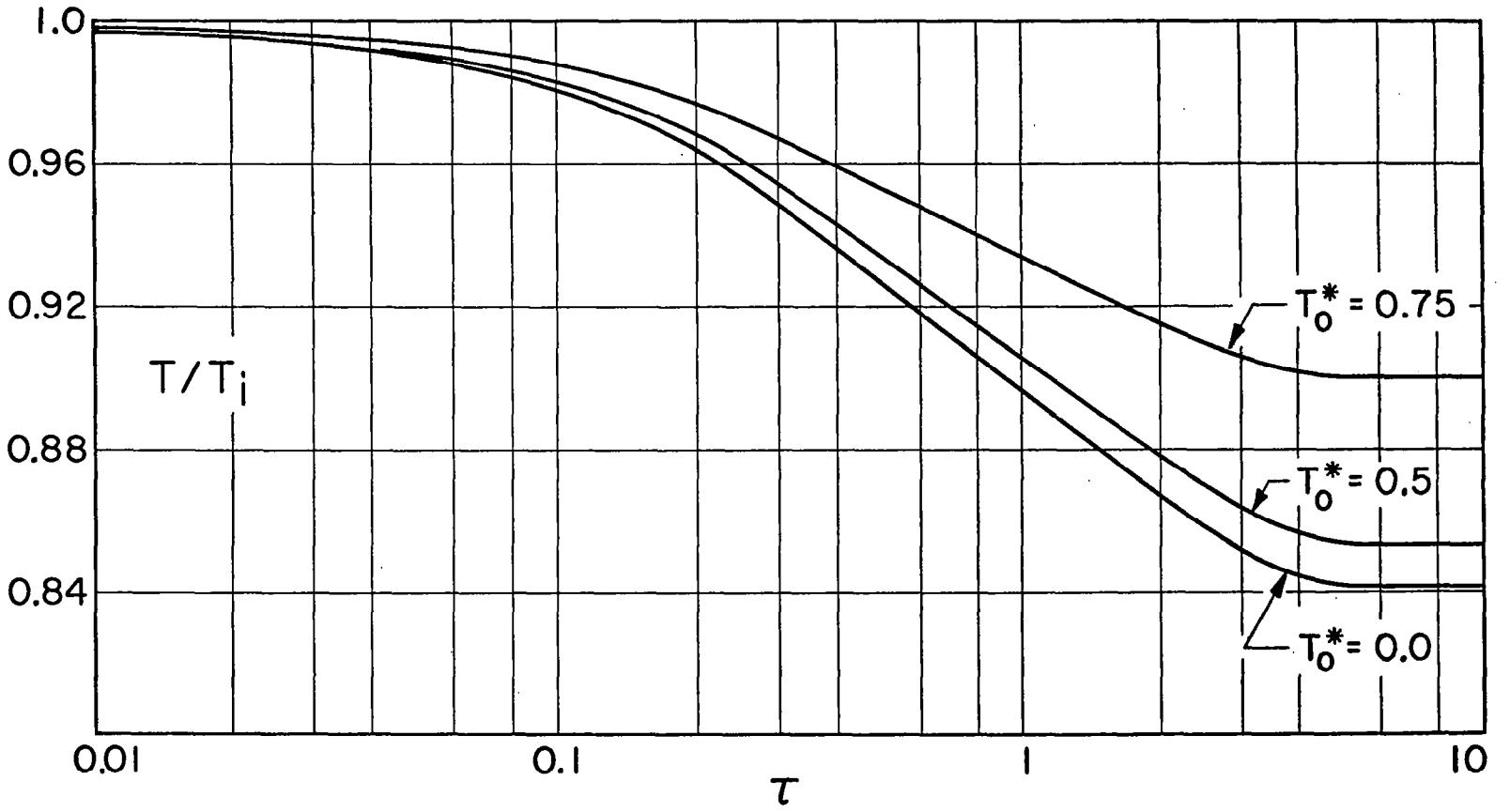

Figure 9

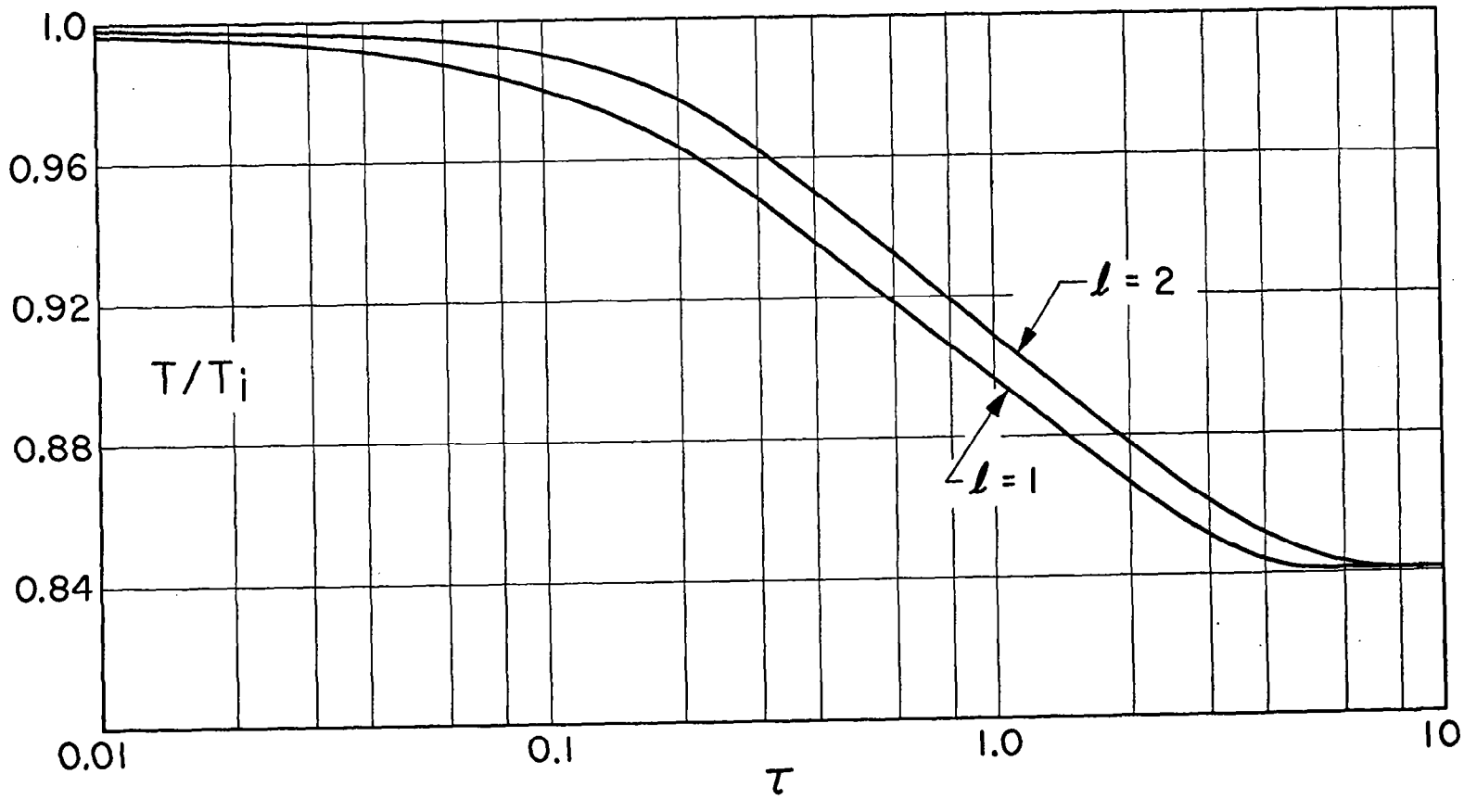

Figure 10

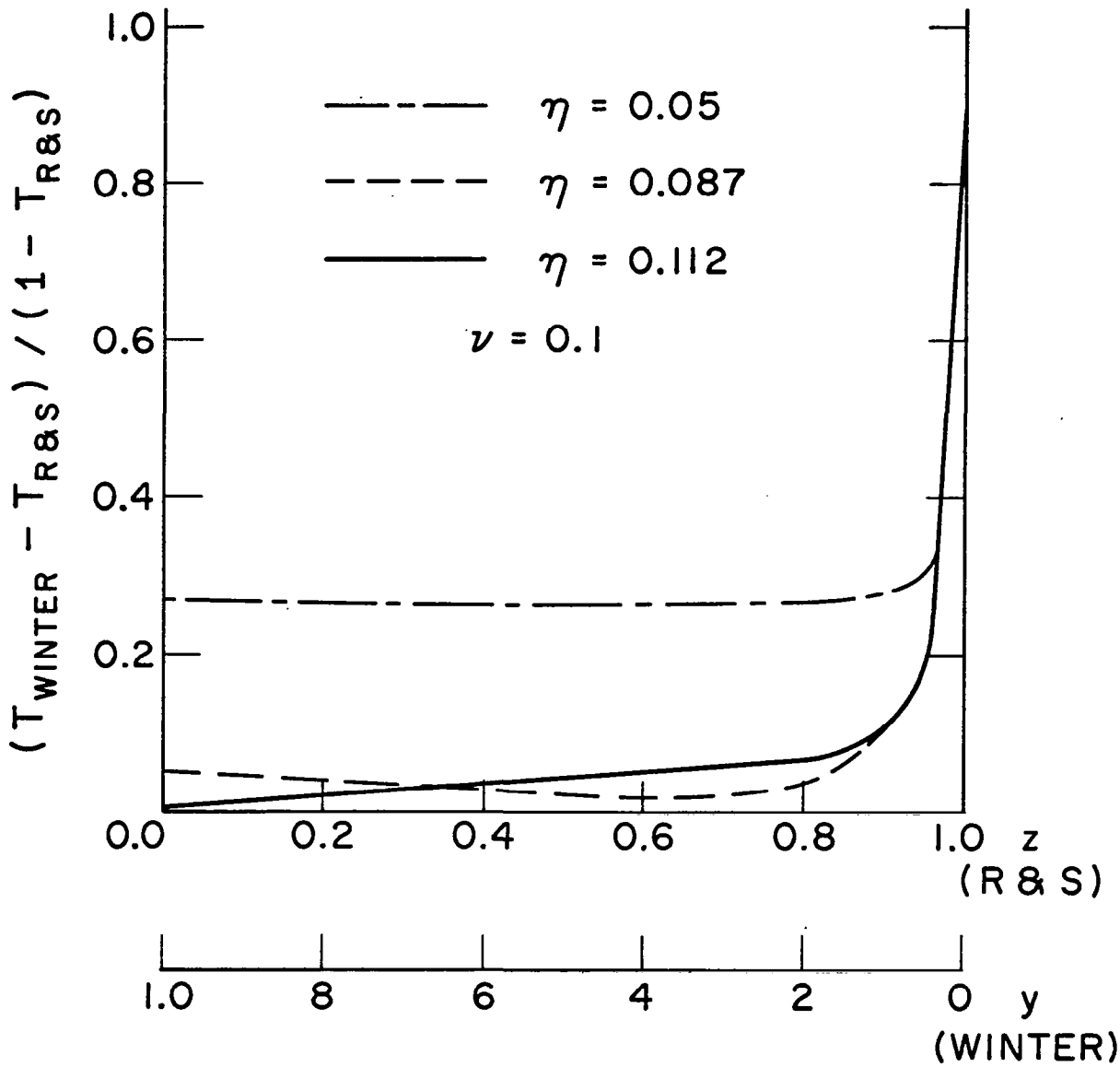

Figure 11

NASA-Langley, 1967 — 12 CR-905